Journal of

Applied and Computational Mechanics

Research Paper

Numerical Analysis of an Edge Crack Isotropic Plate with Void/Inclusions under Different Loading by Implementing XFEM

Achchhe Lal[1] , Manoj B. Vaghela[2] , Kundan Mishra[3]

[1] Department of Mechanical Engineering, S. V. National Institute of Technology, Surat-395007, India, Email: lalachchhe@yahoo.co.in

[2] Department of Mechanical Engineering, S. V. National Institute of Technology, Surat-395007, India, Email: manoj0085@gmail.com

[3] Department of Mechanical Engineering, S. V. National Institute of Technology , Surat-395007, India, Email: mishrakp18@gmail.com

Abstract. In the present work, the effect of various discontinuities like voids, soft inclusions and hard inclusions of the mixed-mode stress intensity factor (MMSIF), crack growth and energy release rate (ERR) of an edge crack isotropic plate under different loading like tensile, shear, combine and exponential by various numerical examples is investigated. The basic formulation is based on the extended finite element method (XFEM) through the M interaction approach using the level set method. The effect of single and multi voids and inclusions with position variation on MMSIF and crack growth are also investigated. The presented results would be applicable to enhancing the better fracture resistance of cracked structures and various loading conditions.

Keywords: XFEM, MMSIF, Void/Inclusion, Edge Crack, Crack Propagation, ERR.

1. Introduction

Materials with different desired properties are being widely used for various engineering applications as automotive, shipbuilding, aerospace and medical equipment, etc. In spite of the advanced production technology and machining process, it is impossible to make a defect-free component for various engineering applications. Materials can have various defects like crack, inclusion, void, hole, flaw and due to this strength of materials drastically degraded which leads to the sudden failure of components. So, it is essential to find large stress at the crack tip and the behavior of crack growth so as to avoid the catastrophic failure of various components.

Furthermore, structures are always subjected to various types of implant loadings such as tensile, shear, combine (a combination of tensile and shear) and exponential loadings. Under the action of such loadings crack propagation behavior is abnormal. Hence the evaluation of crack behavior under such loading conditions is one of the areas of research for higher safety and strength.

The interaction between a crack and inclusion in the material is very important for understanding the fracture behavior and improving the fracture resistance. The crack tip in various engineering materials is affected by the geometry and the stiffness of near second phase inclusions and/or voids. The density and geometry of inclusion, the stiffness ratio between inclusion and voids and materials play a major role to enhance or reduce the stress at the crack tip. Crack-inclusion, interaction studies have great importance to understand the near crack-tip field for the fracture behavior of the material. In this direction, Sih [1] proposed energy field-based theory, where field amplitude is measured as "energy-density factor", S as stress-intensity factor K in classical fracture mechanics. The critical value of S gives information on crack initiation and fracture toughness of materials. The strain energy density theory is also capable to handle a variety of mixed-mode crack problems. Ke and Liu [2] presented strain at the crack tip as fracture criteria for ductile material and is compared to

J-integral and crack surface opening displacement (CSOD) and it is confirmed that CSOD can be used as one of the fracture criteria but the correlation of these criteria with stress intensity factor has not been established. Chien et al [3] applied the superposition of the conventional finite element method on singularity at the crack tip. In this study stress intensity factor at the crack tip of a single edge, the crack plate is calculated and found better accuracy in the results.

Due to some limitations in the conventional finite element, many researchers started giving more interest in XFEM to analyze fracture problems. In this direction, Belytschko et al. [4] developed a better methodology to handle discontinuity by XFEM where discontinuity is incorporated without remeshing and this method is successfully implemented to analyze crack growth in the material under loading. The result obtained from this new methodology is very near to the experimental results. Sukumar and Prevost [5] implemented computer program Dynaflow based on the finite element method, where the 2-D crack in isotropic and biomaterial plate is analyzed by implementing XFEM in finite element code. This method provided a simple platform where discontinuous fields by the partition of unity framework are incorporated in a standard finite element package.

Bellec and Dolbow [6] represented the limitations of XFEM for the representation of discontinuities near the crack tip. Here, they proposed a modified enrichment method in XFEM by using a ramp function. This study has been carried out for the special case where crack approaches the local nodal spacing. Belytscho et al [7] presented the importance of XFEM with level set methods and its applications, especially for complicated geometry, crack growth and moving interface. XFEM has increased the capability of the finite element method to solve the fracture mechanics problems which are very difficult for the conventional finite element method. Asadpoure [8] et al used XFEM for modeling and analysing of 2D orthotropic media where crack–tip displacement fields are added to enrich the finite element with the partition of unity. Here, crack growth is implemented without remeshing and MMSIF is calculated by interaction integral (M-integral). LI and Chen [9] developed formulations for the prediction of the variations of stress intensity factors, where transformation toughening theory is used for the formulation. Mousavi and Sukumar [10] presented the Gaussian integration method to evaluate weak form integrals in XFEM. Here, a point elimination algorithm is adopted, where quadrature has a minimal number of Gauss points. Kumar et al [11] presented a method for investigating dynamic response, where three crack tip enrichment functions are used in XFEM. Here, the Heaviside function with ramp function is utilized and dynamic stress intensity factor is calculated by interaction integral approach. Belytschko and Gracie [12] studied a method to calculate Peach-Koehler force which is based on XFEM where discontinuities have been modeled by Volterra dislocation model for a more complex problem. Sukumar et al [13] presented work on modeling holes and inclusions by level set in XFEM, where they described the modeling the internal boundaries where local enrichment functions in the generalized finite element method for modeling corners in two dimensions are used. Wiroj et al [14] presented adaptive finite element method to determine stress intensity factors K_I and K_{II} of the crack plate with different inclusions where a single edge crack plate of polycarbonate with different discontinuities are considered where it is confirmed that the adaptive finite element method provides a better result as compared to photoelastic technique. Jiang et al [15] discussed the simulation technology by XFEM the component with multiple discontinuities as cracks, voids, and inclusions and predicted the crack path when it interacts with hard and soft inclusions.

Natrajan et al [16] presented a numerical analysis of inclusion crack interaction by XFEM where both inclusion and crack are modeled within the XFEM framework and found better accuracy and flexibility in the results. Sharma [17] studied the crack interaction with discontinuities by XFEM in the solution domain where remeshing is not required. Stress intensity factor (SIF) is calculated by the interaction integral method and the effect of crack orientation under mechanical loading is also considered and it is observed that SIF at the crack tip is decreased with the interaction of hard inclusion. Shedbale based on[18] presented a nonlinear analysis of a plate with crack and multiple discontinuities in-plane stress condition, by considering Von-Mises yield criteria for the elasto-plastic behavior of the plate where it is observed that fatigue life of the plate is drastically affected due to the presence of holes.

Gresa et al. [19] described XFEM as a powerful tool to handle fracture mechanics problems. Here, uncertainty associated with different variables as material properties, external load and geometry are also being considered by the perturbation method and the result obtained by the present method is compared with the Monto Carlo simulation. Khatri and Lal [20] presented stochastic XFEM for fracture analysis and crack propagation in an anisotropic plate with a hole and emerging crack under different in-plane loadings where fracture response is described by means of mean and coefficient of variance. In this study, it is observed that even shorter cracks on the edge of the hole are very sensitive due to high-stress concentration on the crack tip. Khatri and Lal [21] described the stochastic fracture response in an isotropic plate with a circular hole and emerging crack under biaxial loading and mean and coefficient of variance of MMSIF is calculated second-order perturbation technique and it is found that crack propagation direction is much influenced by the applied loadings.

Ebrahimi et al. [22] presented Discrete Crack Dynamics which is based on Multipole Method (MPM) for arbitrarily oriented cracks and inclusions in the brittle material and this method is validated with the result of experimental data and finite element analysis. In this study, it is observed that the present method provides an accurate result for the displacement field, MMSIF and energy release rates of cracks. Huang et al. [23] developed domain-independent interaction integral for the evaluation of dynamic stress intensity factors in bi-materials with crack and inclusion and here it is observed that the present method is more sensitive to the elastic modulus than the density of the inclusion. Yu and Bui [24] presented an effective computational approach based on XFEM for the numerical simulation of material with strong and weak discontinuities and this study has been carried out for multiple crack and inclusion in the material. The results obtained from this method are found to be more accurate, better performance and have low cost for the simulation of 2-D cracks

and inclusions. Zhang et al. [25] presented a distributed dislocation method for the interaction between cracks and inclusions, this method has integral equations with Cauchy kernels and are solved by Gauss–Chebyshev quadrature. The results found from this method are compared and confirmed with finite element analysis results. Singh et al. [26] evaluated the fatigue life of homogeneous plate with multiple discontinuities as cracks, holes, and inclusions under cyclic loading by XFEM and fatigue life is estimated by Paris fatigue crack growth law. Lal et al. [27] evaluated normalized MMSIF by XFEM with second-order perturbation technique (SOPT) and independent Monte Carlo Simulation (MCS) for crack propagation and reliability analysis. In this study it is observed that crack angle, crack length, load, fiber orientation, and lamina thickness are more sensitive than other random system properties for the evaluation of MMSIF. Kumar et al. [28] proposed virtual node XFEM for the analysis of kinked cracks, where the actual tip element is divided into two virtual split and virtual tip element. The proposed method is suitable for the analysis of crack growth in homogeneous and bi-materials. Bui and Zhang [29] presented the stationary dynamic crack analysis through XFEM for 2D homogeneous and piezoelectric material.

Teng et al. [30] investigated the effect of micro cracks on the macro crack propagation by XFEM with adaptive mesh refinement method. It is observed that the present method can accurately calculate SIF for both macro and micro crack tip. Han et al. [31] investigated the Mode I crack propagation under tensile strength through the discrete element method (DEM) bonded particle model and Brazilian indirect tension test. Zhao [32] presented the comparative study among peridynamics (PD) and XFEM by taking various types of crack to study the crack growth. Sun et al. [33] investigated the crack propagation in a reactor pressure vessel by inducing thermal shock by implementing XFEM. Sim and Chang [34] investigated crack growth in the nuclear pipe though XFEM under the thermal aging effect. Wilson et al. [35] proposed the microstructural sensitivity and driving force for crack growth using XFEM and experimental method. M. Surendran et al. [36] investigated the crack propagation using edged based smoothed finite element method (ESFEM) and scaled boundary finite element method (SBFEM). Sun et al. [37] used the cracking element method (CEM) to analyze the behavior of complex crack growth. Funari et al. [38] implemented to predict crack growth by implementing a moving mesh methodology established on Arbitrary Lagrangian Formulation (ALE) strategy. Sosa et al. [39] investigated the energy release rate using XFEM for composite laminates. Roberto and Ma [40] presented the energy release rate for moving circular crack using the M-integral approach. Mesa et al. [41] proposed a "local" hypercomplex-variable finite element method, (L-ZFEM) to determine the energy release rate (ERR) through the stiffness derivative equation.

Patil et al. [42] proposed the multiscale finite element method (MsFEM) with XFEM to evaluate the elastic properties of heterogeneous materials. Feng and Li [43] presented the combined approximations (CA) approach combined with XFEM to evaluate the fatigue crack growth. Feng and Han [44] formulated the multigrid (MG) algorithm combined with XFEM for the fatigue crack growth analysis. Pu and Zhang [45] investigated the generalized dynamic intensity factor, though the XFEM for crack magnetoelectroelastic material. Zhang and Bui [46] presented the combination of XFEM and fictitious crack model to analyze the cohesive crack growth in concrete. Kang et al. [47] proposed an extended 4-node quadrilateral element (XCQ4) for the linear elastic problem of fracture mechanics. Wang et al. [48] presented the 3D inclusions/voids numerical modeling by XFEM. Kang et al. [49] analyzed the dynamic stationary crack for an isotropic and anisotropic material. Kang et al. [50] investigate the quasi-static crack propagation for a plate with crack and hole by finite element method. Wang et al. [51] presented a 3D approach for planar straight and curved crack using the hexahedron element by XFEM. Gu et al. [52] investigated the multi inclusions problems through the extended isogeometric analysis (XIGA) combined with locally refined (LR) B-spline and level set method.

From the above literature review, it is observed that researchers are showing great interest in XFEM based fracture mechanics with the interaction of crack and inclusions/voids. Many researchers had investigated the SIF and crack growth for crack with a void or/and inclusion problem under tensile and shear loading. The scope of work is found for this kind of work under combine and exponential loading to analyze MMSIF, crack growth and Energy Release Rate (ERR) for interaction with crack and single or/and multi voids/inclusions. The contribution of this work is, Investigate the MMSIF, crack growth and ERR study for an edge crack plate with single or/and multi voids/inclusions and by position variation of single or/and multi voids/inclusions under various types of in-plane loadings such as tensile, shear, combine (combination of tensile and shear) and exponential. Evaluate the effect of different loading conditions for the interaction of an edge crack with single or/and multi voids/inclusions for safety and strength of the structure.

In this present work, the main focus is (a) numerical investigation of various discontinuities like crack, voids, soft and hard inclusions interaction in an isotropic plate with an edge crack through implementing XFEM under different loading (tensile, shear, combine and exponential). It is investigated the MMSIF in various case studies, like with a single void/inclusion, multi voids/inclusions and by position variation of voids/inclusions. (b) The analysis of crack propagation behavior with different positions of void/inclusion under different loading. Also (c) investigate the Energy release rate (ERR) with voids/inclusion under different loading for an edge crack isotropic plate.

The paper is organized as follows: section 1 is elaborating on the motivation and literature review related to the fracture behavior of edge crack plate with the interaction of various discontinuities under different loading. In section 2, XFEM formulation of an isotropic plate with edge crack, void, and inclusion and crack growth behavior is given and the MMSIF is calculating for above mention various cases. Then in section 3, the deterministic validation example is performed for MMSIF and ERR. And analyzing some case studies of single/multi void/inclusion, by changing the position of void/inclusion, crack growth behavior and ERR for an edge crack isotropic plate under different loading. At last, in section 4 is providing the conclusion of the present work.
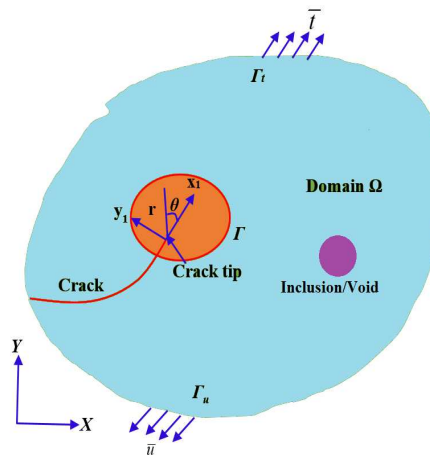
Fig. 1. An arbitrary body with crack and inclusion, subjected to traction $\bar{t}$ and displacement $\bar{u}$, having global Cartesian coordinates (X, Y), local polar coordinates (r, ϑ) defined at the crack-tip surrounded by contour Γ and its interior area A with arbitrary boundary conditions

2. XFEM Formulation

2.1 XFEM Formulation of an edge crack isotropic plate with various discontinuities

Modeling of crack growth in the finite element method is time-consuming and here it's necessary to update meshing at every step of crack growth. In XFEM remeshing is not required during crack growth and discontinuities are modeled by enrichment functions. Sukumar et al. [53] and Stolarska et al. [54] represented the displacement vector in the XFEM framework is given below:

$$u^h(x) = \sum_{i=1}^{n} N_i(x)\bar{u}_i + \sum_{i=1}^{n_c} N_i(x)H(x)a_i + \sum_{i=1}^{n_{t1}} N_i(x)\sum_{\alpha=1}^{4}\Phi_\alpha^1(x)b_i^{\alpha1} + \sum_{i=1}^{n_{t2}} N_i(x)\sum_{\alpha=1}^{4}\Phi_\alpha^2(x)b_i^{\alpha2} + \sum_{i=1}^{n_h} N_i(x)\chi(x)c_i \tag{1}$$

where $\bar{u}_i$, a_i, $b_i^{\alpha1}$, $b_i^{\alpha2}$ and c_i are the conventional degrees of freedom (dofs), and extra dofs is added to crack face, crack tip and for inclusion/void. A body is considered whose area is denoted by Ω and its outer boundary Γ containing a crack and inclusion indicated by Γ_c, as in Fig. 1. The body is experiencing uniform volume/ body loads b, and the surface load or forces are applied at the boundary Γ_t. Over the boundary surface, boundary conditions are applied, Γ_u, where $\Gamma = \Gamma_u + \Gamma_t + \Gamma_c$. The parameter $\bar{u}$ is the displacement and $\bar{t}$ is the tractions. It is assumed that a surface with crack and inclusion is traction free.

Here, a set of nodes in FEM mesh, enrichment due to fully cut the elements by crack, enrichment for the elements at the crack tip, and enrichment for the inclusion are denoted by n, n_c, n_t and n_h respectively. The total dofs is represented as [21]:

$$dofs = size(n) + size(n_c) + size(n_t) + size(n_h) \text{ where, } \mathrm{n_t} = \mathrm{n_{t1}} + \mathrm{n_{t2}} \tag{2a}$$

The parameters $H(x)$ and $\chi(x)$ denote the Heaviside function for the enrichment of crack and inclusion/void which values are +1 or -1. Crack tips asymptotic functions are represented by Φ_α^1 and Φ_α^2. The displacement function or asymptotic function near the crack tip is represented as:

$$\Phi_\alpha^{t1} = \sqrt{r}\sin\left(\frac{\theta}{2}\right), \Phi_\alpha^{t2} = \sqrt{r}\cos\left(\frac{\theta}{2}\right), \ \Phi_\alpha^{t3} = \sqrt{r}\sin\theta\cos\left(\frac{\theta}{2}\right), \Phi_\alpha^{t4} = \sqrt{r}\sin\theta\cos\left(\frac{\theta}{2}\right) \tag{2b}$$

The relationship between MMSIF and J-integral for mixed-mode problems in 2D can be represented as:

$$J = \frac{K_I^2 + K_{II}^2}{E_{eff}} \text{ where, } E_{eff} = \begin{cases} E & \text{for plane stress} \\ \frac{E}{1-\nu^2} & \text{for plane strain} \end{cases} \tag{3}$$

The J integral for the body with crack is given in Eq. (4), where Γ area inside contour W is the strain energy density, δ_{1j} is Kronecker delta, n_j is the outward unit normal to Γ for j^{th} component, σ_{ij} is stress tensor and u_i is displacement field vector. A crack body is denoted by two states and the summation of two states is represented in Eq. (5).

$$J = \int_\Gamma \left(W\delta_{1j} - \sigma_{ij}\frac{\partial u_i}{\partial x_1}\right)n_j d\Gamma \tag{4}$$

$$J^{(1+2)} = \int_{\Gamma} \left[\frac{1}{2} \left(\sigma_{ij}^{(1)} + \sigma_{ij}^{(2)} \right) \left(\varepsilon_{ij}^{(1)} + \varepsilon_{ij}^{(2)} \right) \delta_{1j} - \left(\sigma_{ij}^{(1)} + \sigma_{ij}^{(2)} \right) \frac{\partial (u_i^{(1)} + u_i^{(2)})}{\partial x_i} \right] n_j d\Gamma \tag{5}$$

On further solving, get

$$J^{(1+2)} = J^{(1)} + J^{(2)} + \frac{2}{E_{eff}} (K_I^{(1)} K_I^{(2)} + K_{II}^{(1)} K_{II}^{(2)}) \tag{6}$$

By comparing the Eqs. (3) and (6) get,

$$I^{(1,2)} = \frac{2}{E_{eff}} (K_I^{(1)} K_I^{(2)} + K_{II}^{(1)} K_{II}^{(2)}) \tag{7}$$

where, $I^{(1, \text{Mode I})}$ and $I^{(1, \text{Mode II})}$ are interaction integrals. The SIFin XFEM for two states $K_I^{(1)}$ and $K_{II}^{(1)}$ are evaluating by putting $K_I^{(2)} = 1$ and $K_{II}^{(2)} = 0$ and $K_I^{(2)} = 0$ and $K_{II}^{(2)} = 1$ in Eq. (7), get, presented by Stolarska et al. [54].

$$K_I^{(1)} = \frac{M^{(1, \text{Mode I})} E_{eff}}{2} \qquad \text{and} \qquad K_{II}^{(1)} = \frac{M^{(1, \text{Mode II})} E_{eff}}{2} \tag{8}$$

2.2 Modeling of crack growth

The maximum circumferential (hoop) stress criteria are commonly used for crack growth criteria, which is based on the calculation of MMSIF. In these criteria, it is assumed that the crack initiation starts when hoop stress reaches the critical value and crack propagates in the direction θ_c where $\sigma_{\theta\theta}$ is maximum. The hoop stress in the direction of crack propagation is found by taking shear stress equal to zero presented by Stolarska et al. [34].

$$\left\{ \begin{matrix} \sigma_{\theta\theta} \\ \sigma_{r\theta} \end{matrix} \right\} = \frac{K_I}{\sqrt{2\pi r}} \frac{1}{4} \left\{ \begin{matrix} 3\cos(\theta/2) + \cos(3\theta/2) \\ \sin(\theta/2) + \sin(3\theta/2) \end{matrix} \right\} + \frac{K_{II}}{\sqrt{2\pi r}} \frac{1}{4} \left\{ \begin{matrix} -3\sin(\theta/2) - 3\sin(3\theta/2) \\ \cos(\theta/2) + 3\sin(3\theta/2) \end{matrix} \right\} \tag{9}$$

$$\frac{1}{\sqrt{2\pi r}} = \cos\left(\frac{\theta}{2} \right) \left[\frac{1}{2} K_I \sin\theta + \frac{1}{2} K_{II} (3\cos(\theta) - 1) \right] = 0 \tag{10}$$

The angle of crack propagation θ_c in the tip coordinate system is defined as:

$$K_I \sin(\theta_c) + K_{II}(3\cos(\theta_c) - 1) = 0 \tag{11}$$

By solving the Eq. (11),

$$\theta_c = 2\arctan \frac{1}{4} \left(K_I / K_{II} \pm \sqrt{(K_I / K_{II})^2 + 8} \right) \tag{12}$$

The magnitude of the crack growth da is user-defined and the new coordinates of the crack tips can be written as presented by K. Khatri et al [21],

$$X_{new} = X_{ini} + da\cos(\theta_c) \text{ and } Y_{new} = Y_{ini} + da\sin(\theta_c) \tag{13}$$

3. Results and Discussion

3.1 Validation study

3.1.1 An edge crack isotropic plate under uniaxial tensile loading

An edge crack isotropic plate is considered for the validation study. The geometry of an edge crack isotropic plate under uniaxial tensile loading is shown in Fig. 2. The geometry dimension of this plate is taken 72 mm x 36mm (L x W), crack length ratio $a/W = 0.3, 0.4, 0.5, 0.6$ ($10.8 \leq a \leq 21.6$), polycarbonate material (PSI) is taken with E = 2.50 GPa, $v = 0.38$, tensile stress $\sigma = 1.1$ MPa as taken by Wiroj et al. [14].

For validation purposes, a standard single-edge crack isotropic plate under uniaxial tensile loading is taken with mesh size 45 x 90 and a total of 3916 Q4-elements. By applying XFEM Mode-1 K_I is determined for $a/W = 0.3, 0.4, 0.5, 0.6$ and compare with the result of Wiroj et. al. [14] and the analytical result as shown in Fig. 3. Analytically SIF can be calculated as given by Mohammadi [55],

$$K_1 = \left[1.12 - 0.23\left(\frac{a}{W} \right) + 10.56\left(\frac{a}{W} \right)^2 - 21.74\left(\frac{a}{W} \right)^3 + 30.42\left(\frac{a}{W} \right)^4 \right] \sigma\sqrt{\pi a} \tag{14}$$
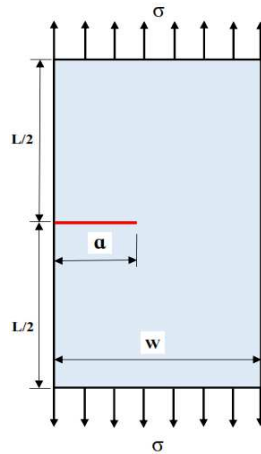
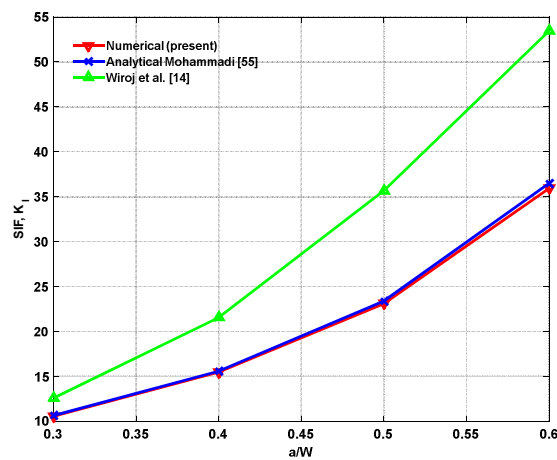**Fig. 2.** An edge crack isotropic plate under uniaxial tensile loading

Fig. 3. A validation graph of SIF K_1 Vs. a/W for an edge crack plate with inclusion under uniaxial tensile loading
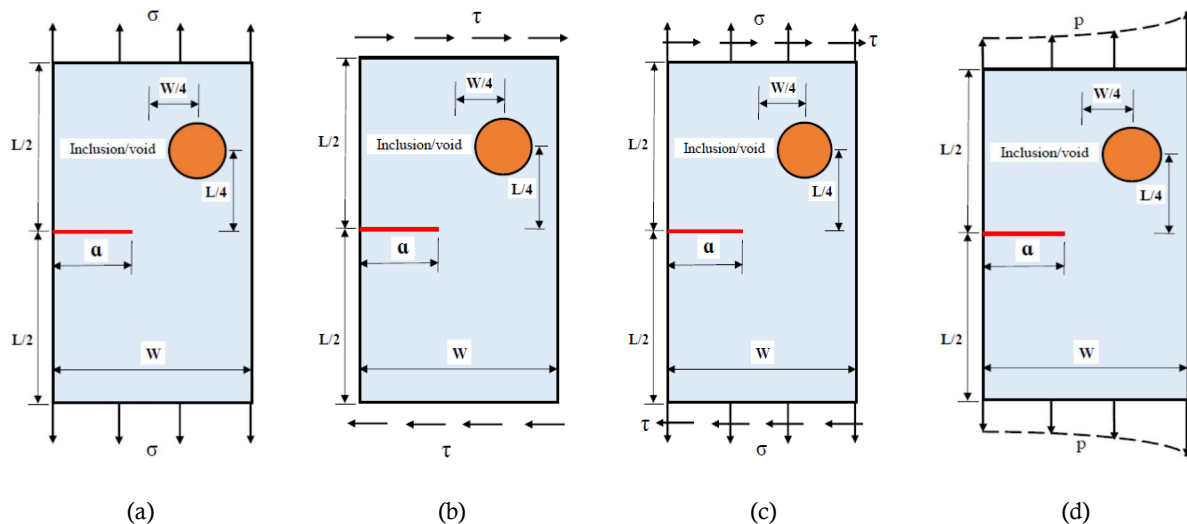

| (a) | (b) | (c) | (d) |

Fig. 4. An edge crack plate with a single inclusion/void under different loading (a-d) Geometry (a) Tensile (b) Shear (c) Combine (d) Exponential

A validation graph shows, results of the present work are very close to the analytical result [55]. The present result is also improved as compared to Wiroj et al. [14] result as shown in Fig. 3. Some cases are solved by using this XFEM mixed-mode, numerical solution for an edge crack isotropic plate with inclusion/void under different loadings.

3.2 Some case studies of an edge crack isotropic plate with inclusion/void under different loadings

3.2.1 An edge crack isotropic plate with a single inclusion/void under different loading

Figs. 4 (a)-(d) show the geometry of an edge crack isotropic plate with a single inclusion/void under different loading.

The geometry dimensions are taken 72 mm x 36 mm (L x W), crack length ratio a/W = 0.2, 0.3, 0.4, 0.5, 0.6 ($7.2 \leq a \leq 21.6$), polycarbonate material (PSI) is taken with E = 2.50 GPa, ν = 0.38. A circular void/soft and hard inclusion is considered with a radius of 6 mm. The position of a void/inclusion is taken at L/4 and W/4 for all cases as shown in Figs. 4 (a)-(d). The soft inclusion is made of Teflon with E_{soft}/E_{PSI} ratio = 0.24 and hard inclusion has taken of AZ61 with E_{hard}/E_{PSI} ratio = 18, tensile stress σ = 1.1 MPa as taken by Wiroj et al. (2011). The shear stress τ = 1.1 MPa considered and in combine stress tensile and shear both are subjected on the plate as shown in Fig. 4 (c). The exponential loading is considered with $p = \sigma \times e^{cx}$, x ($0 \leq x \leq W$) and c = 0.02778.

The same meshing and elements are taken as the above validation problem. MMSIF K_I and K_{II} are determined by XFEM method for various crack length ratios a/W = 0.2, 0.3, 0.4, 0.5, 0.6 as shown in Fig. 5. It is observed that MMSIF K_I and K_{II} increase by the increasing crack length ratio (a/W) for all cases under different loadings. For void, It is found that the MMSIF K_I has increased near to 10% in exponential loading, around 3 times under shear loading and around 4 times under combine loading as compare to tensile loading. For soft inclusion, the MMSIF K_I is found in the same nature and decreases near to 15% as compared to void under different loading. For hard inclusion, the MMSIF K_I is found in the same nature and decreases near to 22% as compared to soft inclusion under different loading, which is due to the strength of the plate increase with the interaction with hard inclusion whereas decreases with the interaction with soft inclusion and void. The SIF K_{II} is found near to zero for tensile and exponential loadings whereas for shear and combined loadings is higher. It is concluded that maximum SIF K_I is found for void and minimum in hard inclusion. So the plate strength is decreased in XFEM fracture behavior for void and it is increasing in XFEM fracture behavior for hard inclusion.
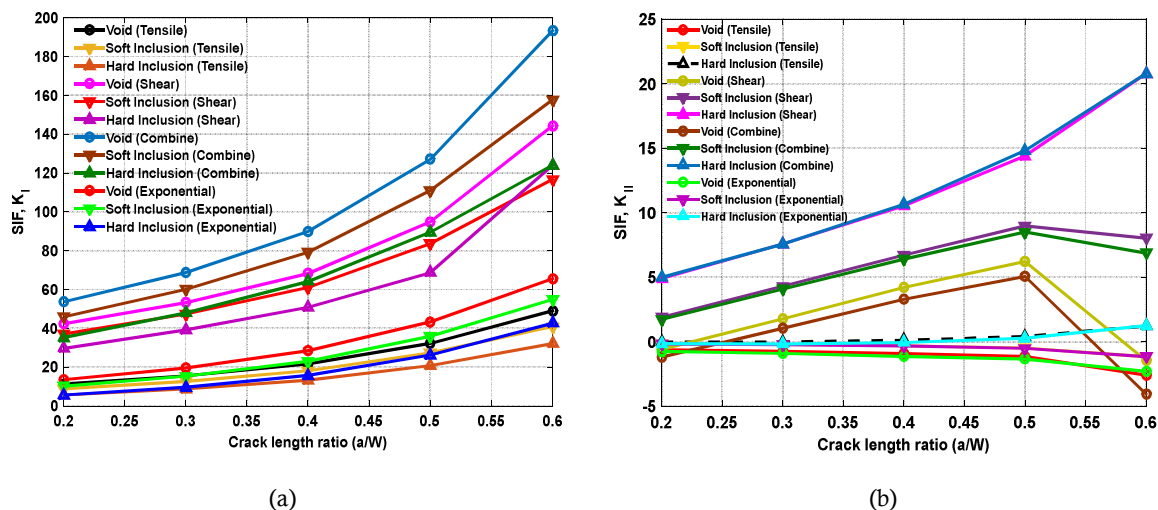

(a)   (b)

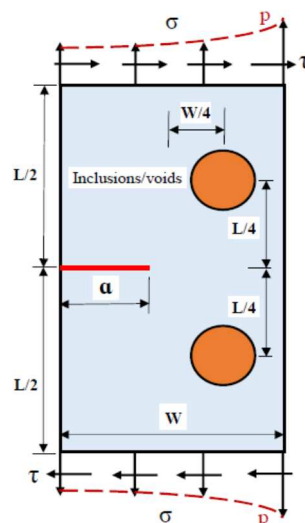**Fig. 5.** MMSIF (a) K_I (b) K_{II} for an edge crack isotropic plate with a single inclusion/void under different loading

Fig. 6. An edge crack plate with 2 inclusions/voids outside under different loading Geometry [Tensile (σ), Shear (τ), Combine (σ and τ both), Exponential (p)]

3.2.2 An edge crack isotropic plate with 2 inclusions/voids outside under different loading

An edge crack isotropic plate with 2 inclusions/voids outside under different loading is shown in Fig. 6. The geometry dimensions (L x W), a/W iterations, meshing and material properties of the plate and inclusions are considered the same

as the previous case with circular void/inclusion of radius 6 mm. The voids/inclusions position is kept outside to crack tip at (L/4, W/4) from the crack tip as shown in Fig. 6. MMSIF through the XFEM is determined under tensile (σ), shear (τ), combine (a combination of σ and τ) and exponential (p) loading. The exponential loading is considered with $p = \sigma\, e^{cx}$, where x varies from $0 \leq x \leq W$ of the plate and c = 0.02778.

MMSIF K_I and K_{II} are determined by XFEM method for various crack length ratios a/W = 0.2, 0.3, 0.4, 0.5, 0.6 as shown in Fig. 7. It is observed that MMSIF K_I and K_{II} are increased by increasing crack length ratio (a/W) for all cases under different loading. For void, It is found that the SIF K_I has increased 15% in exponential loading, around 4 times under shear loading and around 5 times under combine loading as compare to tensile loading. For soft inclusion, the SIF K_I is found in the same nature and decreases near to 5% as compared to void under different loading. For hard inclusion, the SIF K_I is found in the same nature and decreases near to 12% as compared to void under different loading. The SIF K_{II} is found near to zero under tensile and exponential loading, it is found positive increasing mode under shear and combined loading for all cases. It is concluded that maximum SIF K_I is found in the void and minimum in hard inclusion. SIF K_I is also decreased near to 13% as compared to a single void/inclusion case in all cases. Higher SIF K_I is observed for the interaction of plate with a void, this is due to the strength of the plate gets reduced.
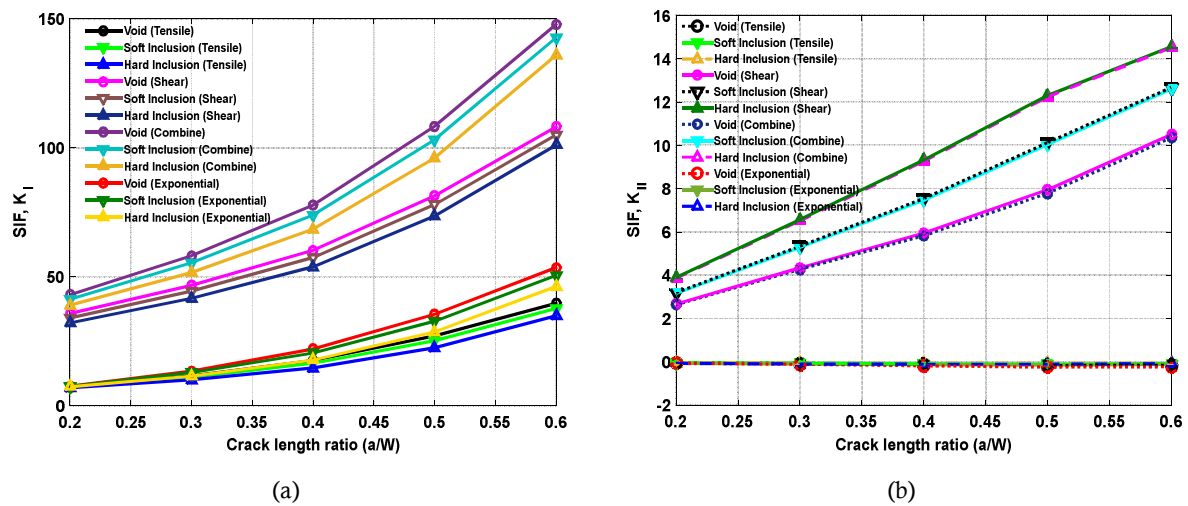

Fig. 7. MMSIF (a) K_I (b) K_{II} for an edge crack isotropic plate with 2 inclusions/voids outside under different loading
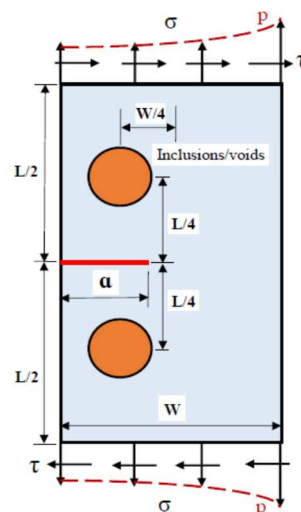

Fig. 8. An edge crack plate with 2 inclusions/voids outside under different loading Geometry [Tensile (σ), Shear (τ), Combine (σ and τ both), Exponential (p)]

3.2.3 An edge crack isotropic plate with 2 inclusions/voids inside under different loading

An edge crack isotropic plate with 2 inclusions/voids inside under different loading is shown in Fig. 8. The geometry (L x W), a/W iterations, circular voids/soft and hard inclusions, radius, meshing and material properties of the plate are considered the same as the previous study. The voids/inclusions position is kept inside at L/4, W/4 from the crack tip as shown in Fig. 8. MMSIF K_I and K_{II} are determined by XFEM for various crack length ratio a/W = 0.2, 0.3, 0.4, 0.5, 0.6 as shown in Fig. 9. It is observed that MMSIF K_I and K_{II} are found in the same nature and increase near to 8% at a/W = 0.2 then it decreased up to a/W = 0.6 as compared to 2 inclusions/voids outside under different loading for all cases.
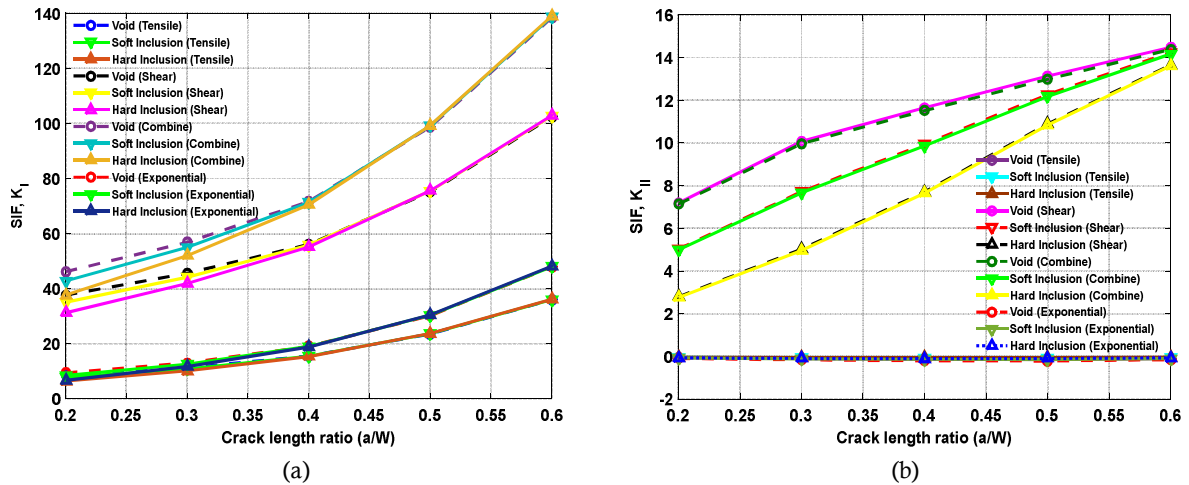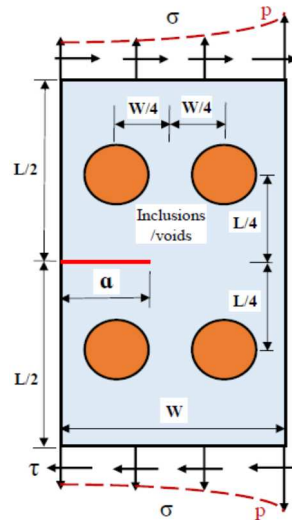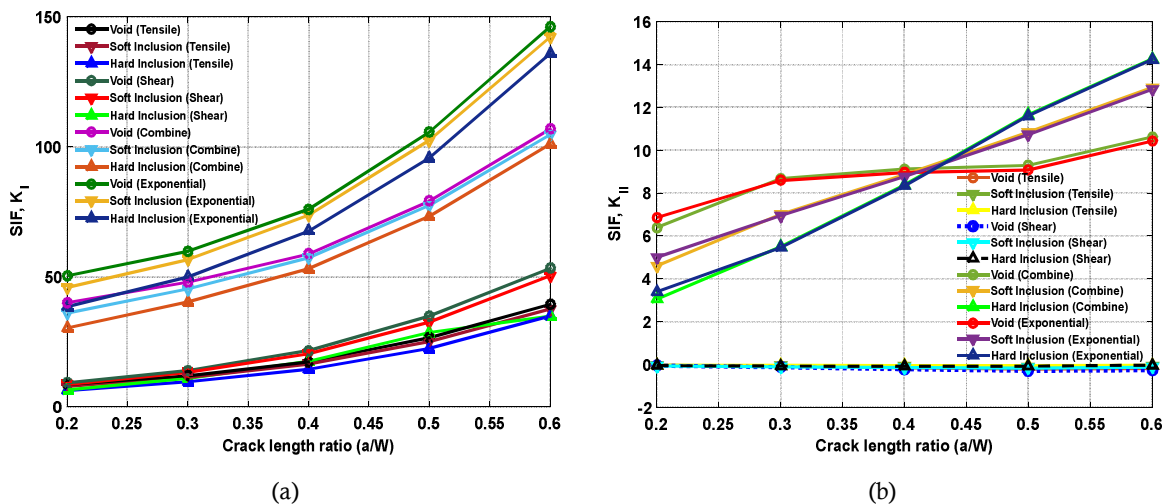
(a)   (b)

Fig. 9. MMSIF (a) K_I (b) K_{II} for an edge crack isotropic plate with 2 inclusions/voids inside under different loading

Fig. 10. An edge crack plate with 4 inclusions/voids under different loading Geometry [Tensile (σ), Shear (τ), Combine (σ and τ both), Exponential (p)]

(a)   (b)

Fig. 11. MMSIF (a) K_I (b) K_{II} for an edge crack isotropic plate with 4 inclusions/voids under different loading

3.2.4 An edge crack plate with 4 inclusions/voids under different loading

An edge crack isotropic plate with 4 inclusions/voids inside under different loading is shown in Fig. 10. The geometry dimensions (L x W), a/W iterations, circular voids/soft and hard inclusions radius, meshing and material properties of the plate and inclusions are considered the same as the previous case. The voids/inclusions position is kept outside and inside to crack tip at L/4 and W/4 as shown in Fig. 10.

MMSIF K_I and K_{II} are determined by XFEM method for various crack length ratios a/W = 0.2, 0.3, 0.4, 0.5, 0.6 as shown

in Fig. 11. It is observed that MMSIF K_I and K_{II} are found in the same nature and increase near to 12% at a/W = 0.2 then it decreased near to 3% up to a/W = 0.6 as compared to 2 inclusions/voids outside under different loading for all cases.

3.3 Some case studies of an edge crack isotropic plate by position variation of inclusions/voids under different loading

3.3.1 An edge crack isotropic plate by position variation of inclusions/voids along with length (L) of the plate

An edge crack isotropic plate with 2 inclusions/voids outside under different loading is shown in Fig. 12. The geometry dimensions (L x W), circular voids/soft and hard inclusions radius, meshing and material properties of the plate and inclusions are considered the same as the previous case. In this case, the MMSIF is determined for a/W = 0.4 and position variation of voids/inclusions L/3, L/4, L/6 and L/9 at W/4 as shown in Fig. 12.
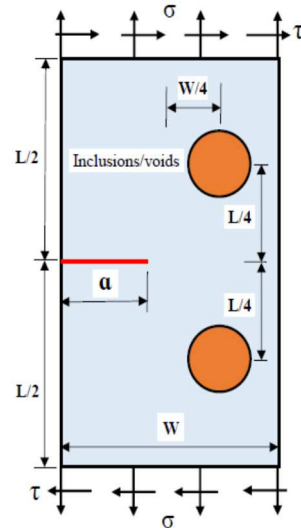
Fig. 12. An edge crack isotropic plate by position variation of 2 inclusions/voids along with length (L) and width (W) under different loading Geometry [Tensile (σ), Shear (τ), Combine (σ and τ both)]
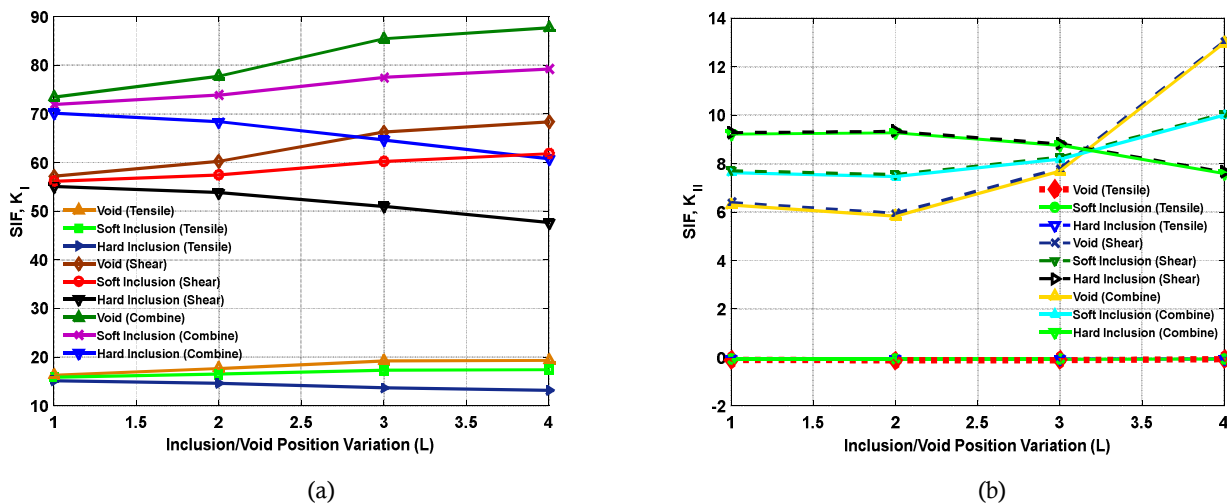

| (a) | (b) |

Fig. 13. MMSIF (a) K_I and (b) K_{II} for an edge crack isotropic plate by position variation of inclusions/voids along with length (L) of the plate

From Fig. 13, it is observed that MMSIF K_I and K_{II} are increased by for L/3 to L/9 under tensile, shear loading and decrease under combine loading. For void, it is found that the MMSIF K_I has first increased near to 9% up to L/6 and then becomes stable at L/9 in tensile, shear and combined loading. For soft inclusion, the MMSIF K_I has first increased near to 4% up to L/6 and then becomes stable at L/9 in tensile, shear and combined loading. For hard inclusion, the SIF K_I has decreased near to 4% for L/3 to L/9 in tensile loading, decreased near to 5% in shear loading and 6% in combine loading. MMSIF K_{II} is found near to zero under tensile loading for all cases, it is found positive increasing mode under shear and combine loading for void and soft inclusion and decrease under shear and combine loading for hard inclusion. It is concluded that maximum SIF K_I is found in the void under combine loading and minimum in tensile loading.

3.3.2 An edge crack plate by position variation of inclusion/void along with width (W) of plate

An edge crack isotropic plate with 2 inclusions/voids outside under different loading is shown in Fig. 12. The geometry dimensions (L x W), circular voids/soft and hard inclusions radius, meshing and material properties of the plate and

inclusions are considered the same as the previous case. In this case, the MMSIF is determined for a/W = 0.4 and position variation of voids/inclusions W/3, W/4, W/6 and W/9 at L/4 as shown in Fig. 12.

From Fig. 14, it is observed that MMSIF K_I and K_{II} remain stable form W/4 to W/9 under tensile, shear and combine loading. For void, the SIF K_I has found maximum at W/3 and then becomes stable from W/4 to W/9 in shear, combine loading and minimum at W/3 then increase and become stable in tensile loading. For soft inclusion, the SIF K_I has observed in the same nature as compared to the void, but in this case maximum, K_I is less as compare to void. For hard inclusion, the MMSIF K_I has observed little decreased up to W/4 and then becomes near to linear under tensile, shear and combined loading. The SIF K_{II} is found in the zigzag mode under tensile loading and decreasing mode under shear and combine for the void. It is found increasing mode up to W/6 and then decreases under tensile loading for soft inclusion. And observed decreasing mode under shear and combine loading for soft inclusion and hard inclusion. It is concluded that maximum SIF K_I is found in the void under combine loading and minimum in tensile loading.
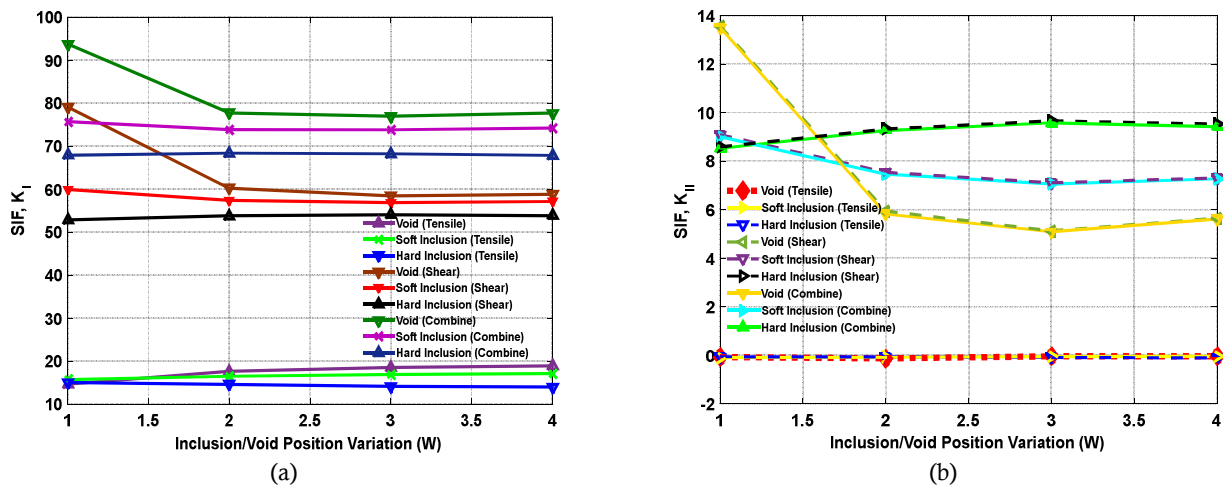

(a)   (b)

Fig. 14. MMSIF (a.) K_I (b.) K_{II} for an edge crack isotropic plate by position variation of inclusions/voids along with width (W) of the plate

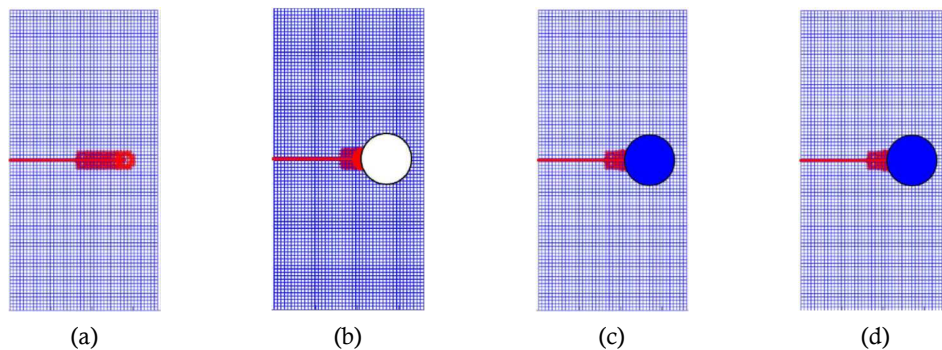(a)   (b)   (c)   (d)

Fig. 15. Crack propagation in an edge crack plate under tensile loading for the aligned position of
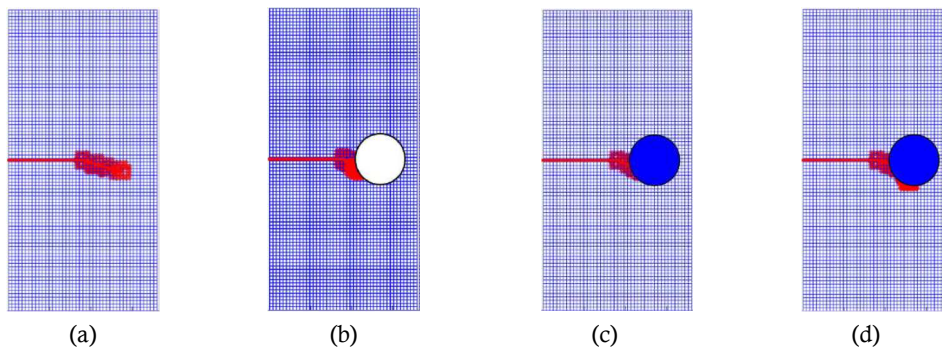(a) without inclusion/void (b) void (c) soft inclusion (d) hard inclusion

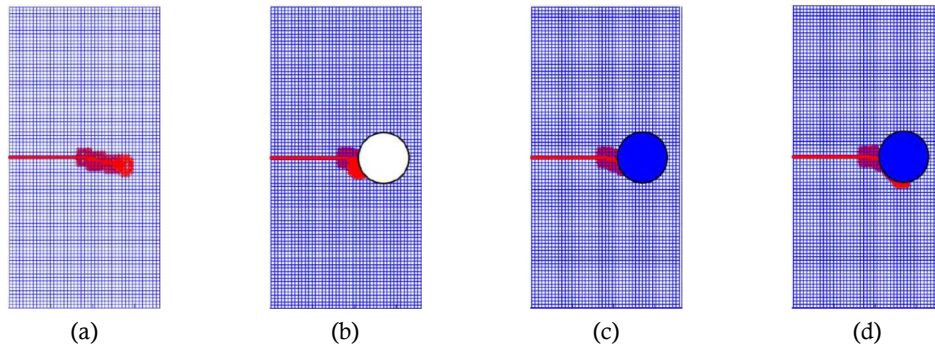(a)   (b)   (c)   (d)

Fig. 16. Crack propagation in an edge crack plate under shear loading for the aligned position of
(a) without inclusion/void (b) void (c) soft inclusion (d) hard inclusion

3.4 The crack growth behavior of an edge crack isotropic plate without and with single inclusion/void under different loading

In this case, analyze the crack propagation behavior and determine the MMSIF K_I and K_{II} using XFEM for an edge

crack isotropic plate for the position of one void and inclusion is aligned, above and below with respect to edge crack. Edge crack plate without void and inclusion is also evaluating the same and compare others. These cases are evaluated under tensile, shear, combine (tensile and shear) and exponential loading conditions. The plate dimensions, material properties, and mashing are taken the same as the validation problem. A circular void, soft and hard inclusion is taken with radius 6 mm. The material properties for soft inclusion and hard inclusion is $E_{soft}/E_{plate}= 0.24$ and $E_{hard}/E_{plate} = 18$ respectively, load value for tensile $\sigma = 1.1$ MPa and shear $\tau = 1.1$ MPa is considered. Edge crack length ratio $a/w = 0.5$ is taken for all cases. To check the behavior of the crack growth path and direction, go up to 6 iterations with a growth step increment of 2 mm.

| (a) | (b) | (c) | (d) |

Fig. 17. Crack propagation in an edge crack plate under combine loading for the aligned position of
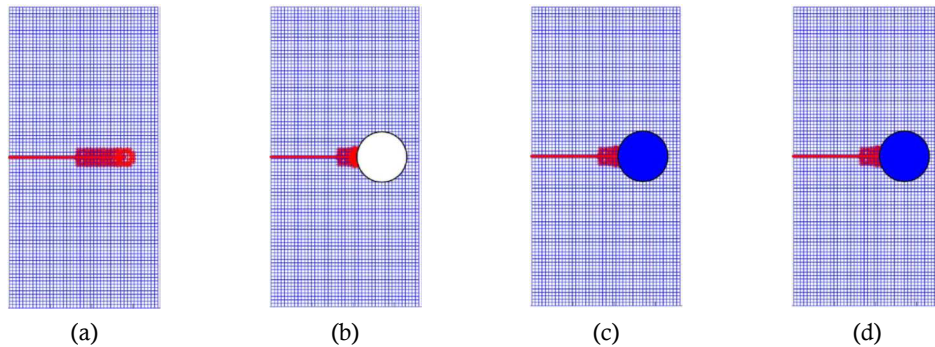(a) without inclusion/void (b) void (c) soft inclusion (d) hard inclusion

| (a) | (b) | (c) | (d) |

Fig. 18. Crack propagation in an edge crack plate under exponential loading for the aligned position
of (a) without inclusion/void (b) void (c) soft inclusion (d) hard inclusion

3.4.1 Without and with single inclusion/void aligned with edge crack under different loading

3.4.1.1 A single inclusion/void aligned the edge crack under tensile loading

Figs. 15 (a)-(d) shows the crack propagation path behavior for an edge crack isotropic plate under tensile loading for without void and inclusion and for the aligned position of a void, soft inclusion and hard inclusion respectively. It is seen that crack growth direction is found linear line along with x-axis in all four cases under tensile loading.

Figs. 19 (a)-(b) present the crack propagation behavior in an edge crack plate with-it and with void and inclusion under different loading for various positions through the MMSIF K_I and K_{II}. It is observed that under tensile loading for without void and inclusion case crack propagation is going continuously liner and SIF K_I is increased for each growth step and maximum can get at the last step. Same crack growth behavior found for soft inclusion. For void, SIF K_I value is a very minor decrease after 1st crack growth step and from the 3rd step it's found zero due to the distance between the crack tip and void periphery is 3mm. In hard inclusion, SIF K_I gets maximum at 3rd crack growth step than decrease and again it will increase gradually. SIF K_{II} is settled on nearest to zero for all cases under tensile loading.

3.4.1.2 A single inclusion/void aligned the edge crack under shear loading

Figs. 16 (a)-(d) shows the crack propagation path behavior for an edge crack isotropic plate under shear loading for without void and inclusion and for the aligned position of the void, soft inclusion, and hard inclusion respectively. It is seen that crack propagation is deviate gradually downward in linear shape for without void and inclusion case, for void and soft inclusion downward in curve shape and for hard inclusion closer curve shape observed under shear loading.

As per Figs. 19 (a)-(b), it is determined that under shear loading for without void and inclusion case SIF K_I is increased for each growth step. For void, SIF K_I value is increased and from the 3rd step, it's found zero due to the distance between the crack tip and void periphery is 3mm. For soft inclusion, SIF K_I gets maximum at 2nd crack growth step than decrease and again it will increase gradually. In hard inclusion, SIF K_I suddenly increases at 2nd crack growth step than decreases and again from the 5th step increase and gets maximum at the 6th step. SIF K_{II} is gradually decreased for without void and inclusion and for soft inclusion, increase for the void, in hard inclusion decreasing and increasing type zigzag pattern got and at 3rd step suddenly increased and 6th step decreased due to get hard material after 2nd crack growth step.
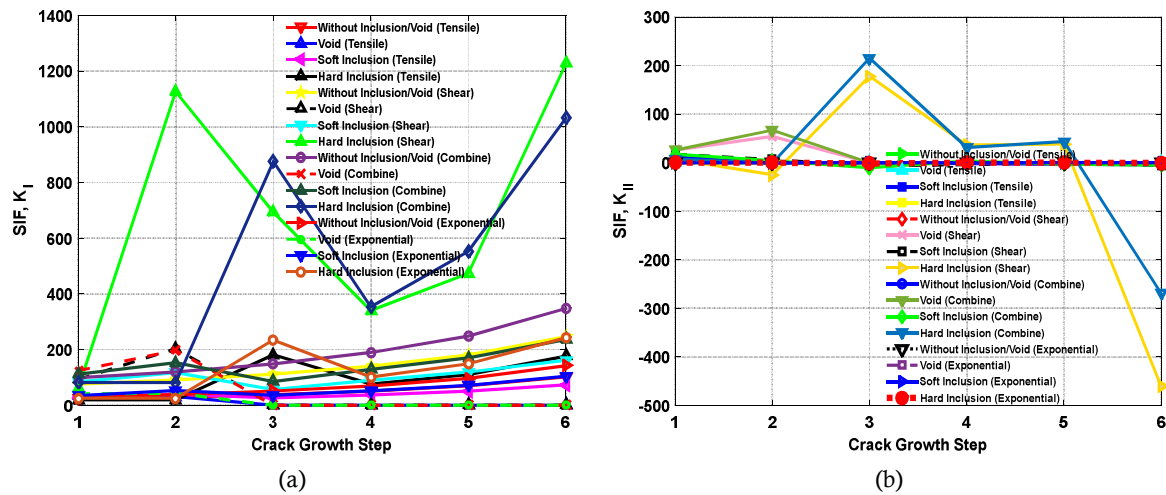
(a)   (b)

Fig. 19. Crack propagation behavior in an edge crack plate without and with void and inclusion under different loading for an aligned position through the MMSIF (a) K_I (b) K_{II}
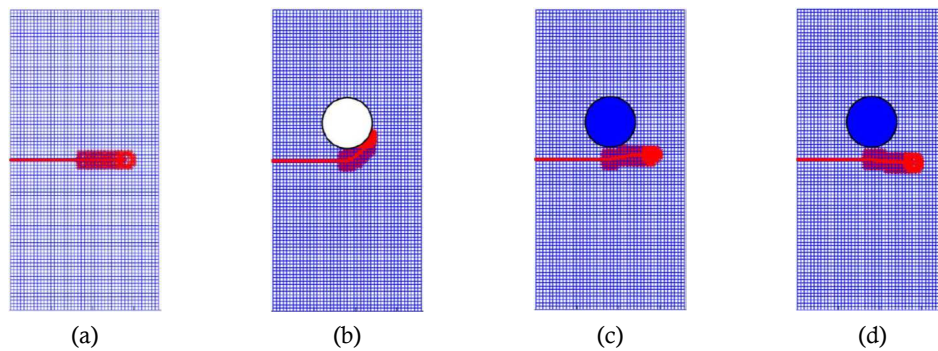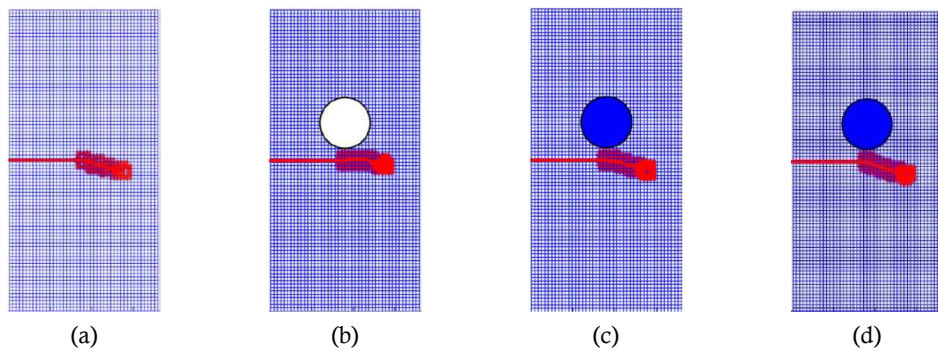

(a)   (b)   (c)   (d)

Fig. 20. Crack propagation in an edge crack isotropic plate under tensile loading for the above position of (a) without inclusion/void (b) void (c) soft inclusion (d) hard inclusion
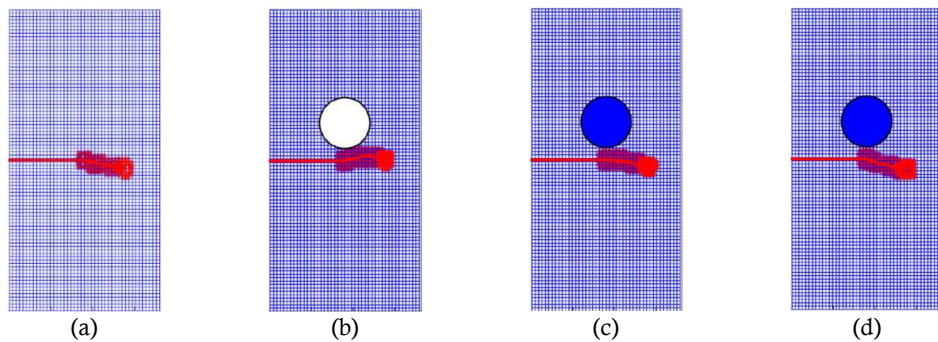

(a)   (b)   (c)   (d)

Fig. 21. Crack propagation in an edge crack isotropic plate under shear loading for the above position of (a) without inclusion/void (b) void (c) soft inclusion (d) hard inclusion

(a)   (b)   (c)   (d)

Fig. 22. Crack propagation in an edge crack isotropic plate under combine loading for the above position of (a) without inclusion/void (b) void (c) soft inclusion (d) hard inclusion

3.4.1.3 A single inclusion/void aligned the edge crack under combined loading

Figs. 17 (a)-(d) shows the crack propagation path behavior for an edge crack isotropic plate under combine loading for without void and inclusion and for the aligned position of the void, soft inclusion, and hard inclusion respectively. It is observed that crack propagation behavior gets very nearer to shear loading because the combined load is considered as a combination of tensile and shear loading.

As per Figs. 19 (a)-(b), it is determined that under combine loading nearest behavior of shear loading is found for MMSIF K_I and K_{II} of all above cases only numerical value of MMSIF K_I and K_{II} is decreased as compared to shear loading due to tensile loading is also subjected with shear loading in combine loading.

3.4.1.4 A single inclusion/void aligned the edge crack under exponential loading

Figs. 18 (a)-(d) shows the crack propagation path behavior for an edge crack isotropic plate under exponential loading for without void and inclusion and for the aligned position of the void, soft inclusion and hard inclusion respectively. It is observed that crack propagation behavior gets very near to tensile loading.

As per Figs. 19 (a)-(b), it is determined that under exponential loading nearest behavior of tensile loading is found for MMSIF K_I and K_{II} of all the above cases the only numerical value of SIF K_I and K_{II} is increased as compared to tensile loading.

As shown in Figs. 19 (a), in hard inclusion under shear loading, SIF K_I suddenly increases at 2nd crack growth step due to crack is just trying to penetrate in hard inclusion than once crack propagate outside to hard inclusion then decrease and again from 5th step increase and get maximum at the 6th step

3.4.2 A single inclusion/void above the edge crack under different loading

3.4.2.1 A single inclusion/void above the edge crack under tensile loading

Figs. 20 (a)-(d) shows the crack propagation path behavior for an edge crack isotropic plate under tensile loading for without void/ inclusion, above the position of the void, soft inclusion, and hard inclusion respectively. It is seen that the crack propagates, to the horizontal linear path in without void/inclusion, to curve path towards the above crack propagate in the void, too little curve towards the above and again linearly crack propagation in soft inclusion, to little curve towards the below and again linearly crack propagate in hard inclusion.

Figs. 24 (a)-(b) present the crack propagation behavior in an edge crack isotropic plate without and with void/ inclusion under different loading for its above position through the   MMSIF K_I and K_{II}. It is observed that under tensile loading for without void and inclusion SIF K_I is gradually increased for each growth step and maximum can get at the last step. Same crack growth behavior found for soft and hard inclusion. For void SIF K_I is increased up to 4th step and after that suddenly decreases and reaches up to zero. SIF K_{II} is settled on nearest to zero in zigzag mode for without void/inclusion and hard inclusion, its increase up to 3rd step, then suddenly decrease (minimum) at the 4th step, then again get zero for remaining step for void, minimum at beginning then increase get the maximum at 4th step and again decrease in soft inclusion.

3.4.2.2 A single inclusion/void above the edge crack under shear loading

Figs. 21 (a)-(d) shows the crack propagation behavior for an edge crack isotropic plate under shear loading for without void/ inclusion and for the above position of the void, soft inclusion, and hard inclusion respectively. It is seen that crack growth is deviated gradually downward in linear shape for without void and inclusion, soft inclusion and hard inclusion. And crack propagates to upward in little curve shape and downward in the linear shape void.

As per Figs. 24 (a)-(b), it is observed that under shear loading SIF K_I is increased for each growth step and found maximum at the last step in all cases. SIF K_{II} gradually decreases at each step without void/inclusion, soft and hard inclusion and found maximum at the beginning and minimum at the end. While for the void first increase then after the 3rd step decreases up to end and found maximum at 3rd step and minimum at the 6th step.

3.4.2.3 A single inclusion/void above the edge crack under combined loading

Figs. 22 (a)-(d) shows the crack propagation behavior for an edge crack isotropic plate under combine loading for without void and inclusion and for the above position of the void, soft inclusion, and hard inclusion respectively. It is observed that crack propagation behavior gets very nearer to shear loading because the combined load is considered a combination of tensile and shear loading.

As per Figs. 24 (a)-(b), it is determined that under combine loading nearest behavior of shear loading is found for MMSIF K_I and K_{II} of all above cases only numerical value of SIF K_I and K_{II} is increase, as compared to shear loading due to tensile loading, is also subjected with shear loading in combine loading.

3.4.2.4 A single inclusion/void above the edge crack under exponential loading

Figs. 23 (a)-(d) shows the crack propagation path behavior for an edge crack isotropic plate under exponential loading for without void/inclusion and for the above position of the void, soft inclusion and hard inclusion respectively. It is seen that crack propagation behavior gets very near to tensile loading.
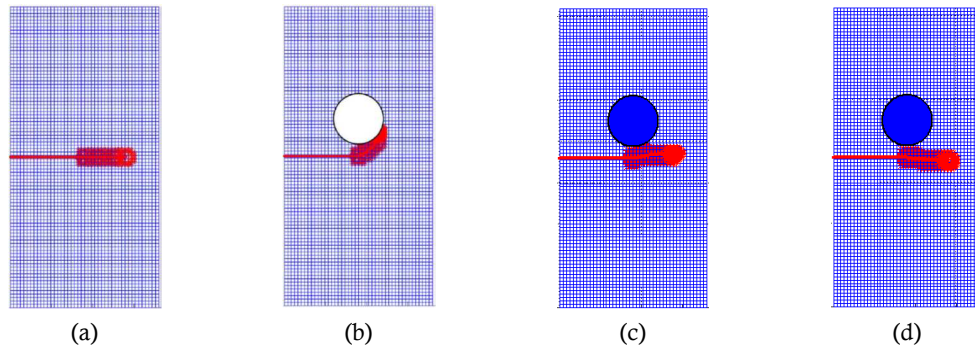
Fig. 23. Crack propagation in an edge crack isotropic plate under exponential loading for the above position of (a) without inclusion/void (b) void (c) soft inclusion (d) hard inclusion
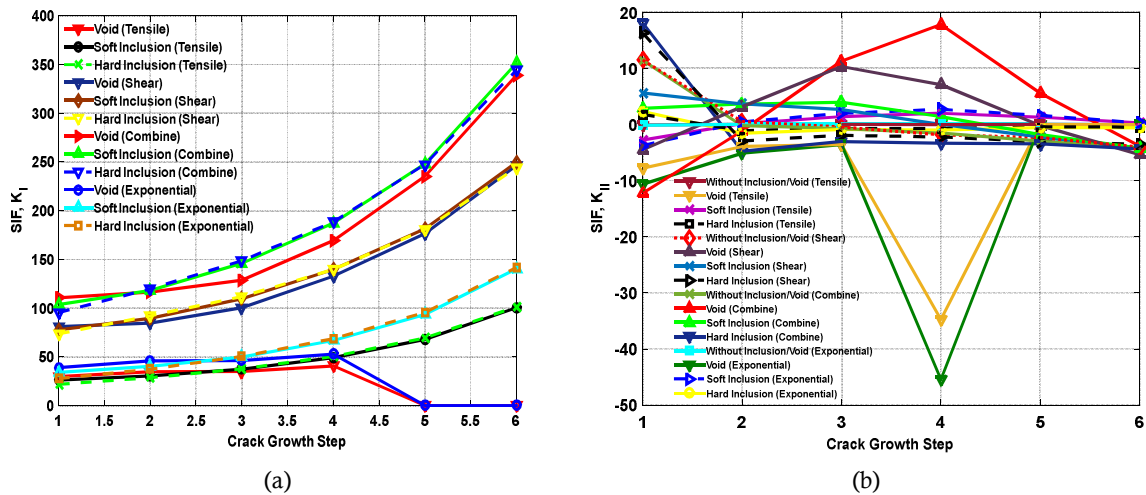

Fig. 24. Crack propagation behavior in an edge crack isotropic plate without and with void and inclusion under different loading for the above position through the MMSIF, (a) K_I (b) K_{II}
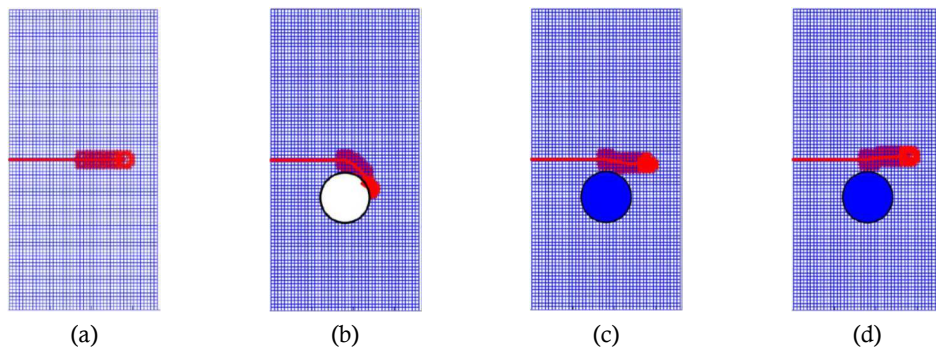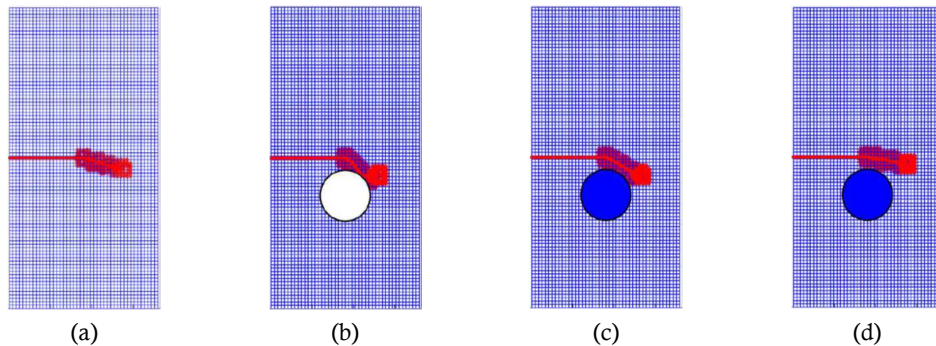

Fig. 25. Crack propagation in an edge crack isotropic plate under tensile loading for below position of (a) without inclusion/void (b) void (c) soft inclusion (d) hard inclusion

Fig. 26. Crack propagation in an edge crack isotropic plate under shear loading for below position of (a) without inclusion/void (b) void (c) soft inclusion (d) hard inclusion
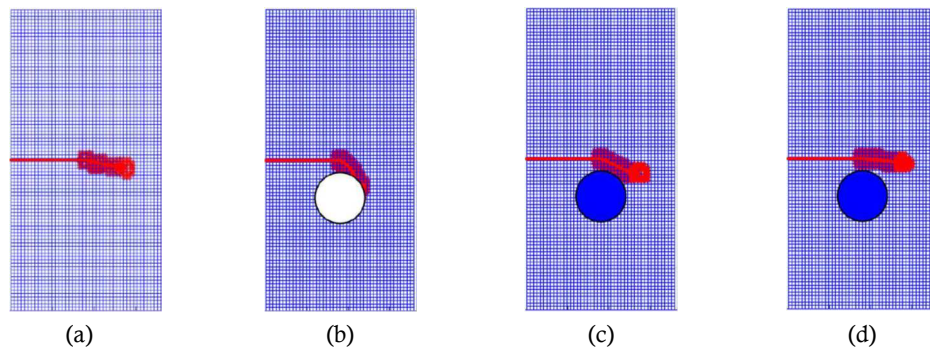
Fig. 27. Crack propagation in an edge crack isotropic plate under combine loading for below
position of (a) without inclusion/void (b) void (c) soft inclusion (d) hard inclusion

As per Figs. 24 (a)-(b), it is observed that under exponential loading nearest behavior of tensile loading is found for MMSIF K_I and K_{II} of all the above cases the only numerical value of SIF K_I and K_{II} is increased as compared to tensile loading. As shown in Fig. 24 (a), in the void under exponential loading, SIF K_I increasing up to 4th crack growth, from the 5th step SIF K_I is reach at zero due to crack is penetrated in the void.

3.4.3 A single inclusion/void below the edge crack under different loading

3.4.3.1 A single inclusion/void below the edge crack under tensile loading

Figs. 25 (a)-(d) shows the crack propagation behavior for an edge crack isotropic plate under tensile loading for without void/ inclusion, below the position of the void, soft inclusion, and hard inclusion respectively. It is seen that the crack propagate, to the horizontal linear path in without void/inclusion, to curve path towards the below crack propagate in the void, to little curve towards the above and again linearly crack propagate in soft inclusion, to little curve towards the above and again linearly crack propagate in hard inclusion.

Figs. 29 (a)-(b) present the crack propagation behavior in an edge crack isotropic plate without and with void/ inclusion under different loading for it's below position through the MMSIF K_I and K_{II}. It is observed that under tensile loading for without void/ inclusion SIF K_I is gradually increase for each growth step and maximum can get at the end. Same crack growth behavior found in soft and hard inclusion. For void SIF K_I is increased and decrease in zigzag mode and found minimum at the 5th step and suddenly increase and get maximum at the end. SIF K_{II} is settled on nearest to zero in zigzag mode for without void/inclusion and hard inclusion, its decrease up to 3rd step than increase (maximum) at 5th step again suddenly decrease (minimum), minimum at beginning, then increase get maximum at 4th step and again decrease for void, maximum at beginning than decrease and get minimum at 4th step and again decrease in soft inclusion.

3.4.3.2 A single inclusion/void below the edge crack under shear loading

Figs. 26 (a)-(d) shows the crack propagation behavior for an edge crack isotropic plate under shear loading for without void/ inclusion and for below position of the void, soft inclusion and hard inclusion respectively. It is seen that crack growth is deviated gradually downward in linear shape for without void and inclusion, soft inclusion and hard inclusion. And crack propagates to downward in little curve shape and upward in linear shape for the void.

As per Figs. 29 (a)-(b), it is observed that under shear loading SIF K_I is increased for each growth step and found maximum at the last step for without void/inclusion, soft and hard inclusion. In the void, it's increasing and get the maximum at 4th step, then again decreases up to the end. SIF K_{II} gradually decreases at each step without void/inclusion, soft and hard inclusion and found maximum at the beginning and minimum at the end. While for the void first decrease up to 4th than increase up to the last step.

3.4.2.3 A single inclusion/void above the edge crack under combined loading

Figs. 27 (a)-(d) shows the crack propagation behavior for an edge crack isotropic plate under combine loading for without void and inclusion and for below position of the void, soft inclusion and hard inclusion respectively. It is observed that crack propagation behavior gets very nearer to shear loading because the combined load is considered a combination of tensile and shear loading.

As per Figs. 29 (a)-(b), it is determined that under combine loading nearest behavior of shear loading is found for MMSIF K_I and K_{II} for without void/inclusion and hard inclusion. It is decreasing up to 3rd step than increase and get the maximum at 4th step, then again decrease for the void, maximum at the beginning than decrease (minimum) at the 4th step and again increase in soft inclusion.

3.4.3.4 A single inclusion/void below the edge crack under exponential loading

Figs. 28 (a)-(d) shows the crack propagation path behavior for an edge crack isotropic plate under exponential loading for without void/inclusion and for the above position of the void, soft inclusion and hard inclusion respectively. It is seen that crack propagation behavior gets very near to tensile loading.
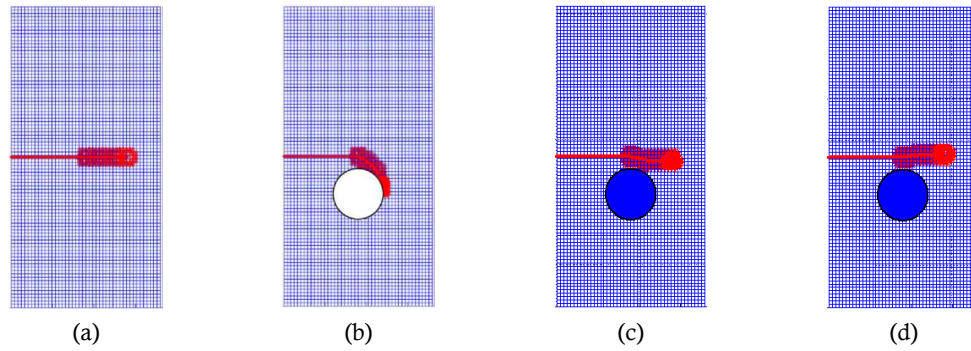
Fig. 28. Crack propagation in an edge crack isotropic plate under exponential loading for the above position of (a) without inclusion/void (b) void (c) soft inclusion (d) hard inclusion
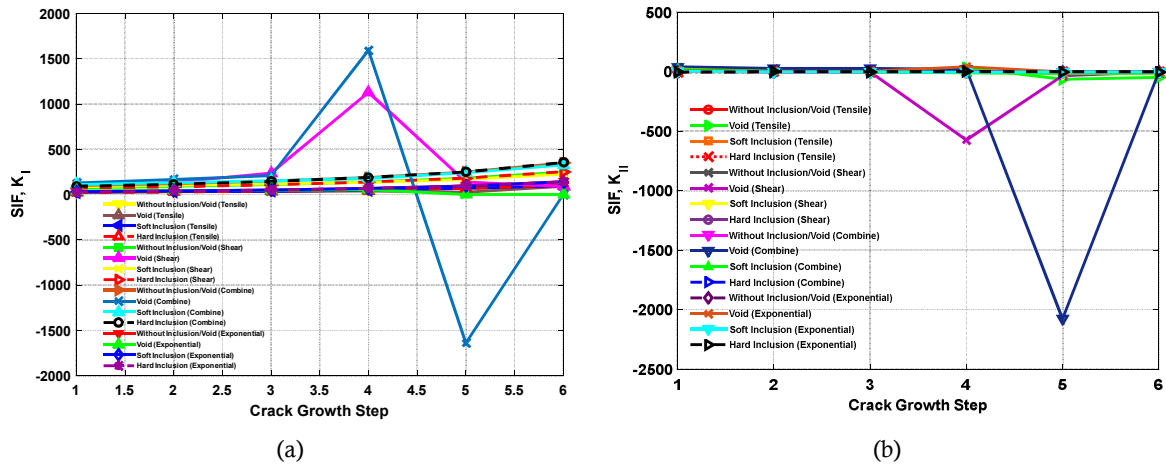

(a)   (b)

Fig. 29. Crack propagation behavior in an edge crack isotropic plate without and with void and inclusion under different loading for below position through the MMSIF (a) K_I (b) K_{II}
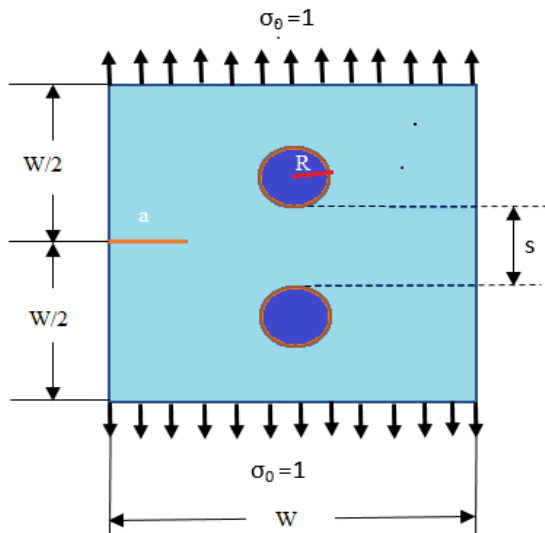

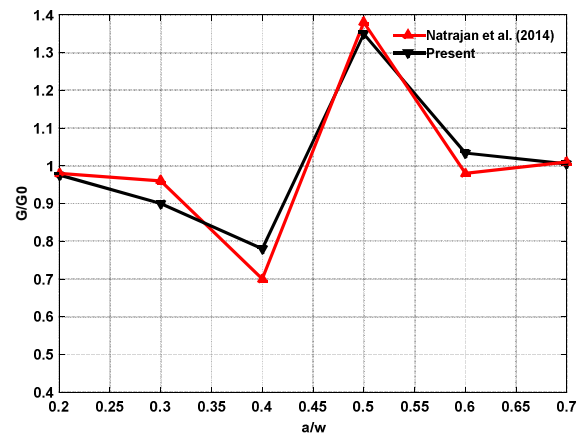**Fig. 30.** Isotropic square plate with edge crack and inclusion under tensile loading

Fig. 31. Validation study of NERR w.r.t. a/W for tensile loading

As per Figs. 29 (a)-(b), it is observed that under exponential loading nearest behavior of tensile loading is found for MMSIF K_I and K_{II} of all below cases the only numerical value of MMSIF K_I and K_{II} is increased as compared to tensile loading. As shown in Fig. 29 (a), in the void, under shear loading, SIF K_I is increasing and get the maximum at 4th step due to crack is trying to deviate toward the void but not penetrating and reach near to void so SIF K_I is suddenly decreased at 5th step and again its increase up to end.

3.5 The energy release rate (ERR) study of an edge crack isotropic plate without and with 2 inclusions/voids under different loading

The energy release rate Go is the rate at which energy is consumed as the material under fracture without

inclusion/void, and is expressed as energy-per-unit-area. It is understood as the decrement in total potential energy as an increment in fracture. Fig. 30 shows an edge crack isotropic plate with inclusions/voids under different loadings. Normalized energy release rate (NERR) is defined as the ratio of energy released of the crack plate with inclusion and without inclusion and/or void represented as (G/Go). Mathematically, the energy release rate is defined as:

$$G = \frac{(k+1)}{8\mu}\left(K_I^2 + K_{II}^2\right) \tag{15}$$

where, k (kolosov coefficient) = $(3 - 4\nu)$, for plane strain, and μ= E $(2+2\nu)$. The ERR is examined for an isotropic square plate with edge crack and two inclusions under tensile loading as shown in Fig. 30.

Here, W=100, E=1 (Plate), E=10^4 (Inclusion), R=W/20 (Radius of Inclusion), X_c=L/2 (Centre of inclusion along the width) and s/W= 0.125 are considered for the validation study for NERR. Fig. 31 shows the validation study of the isotropic plate with edge crack and inclusions under tensile loading for NERR with respect to (w.r.t.) a/W, and the result of the present work is very close to the reference [16] with a maximum variation of 11%.
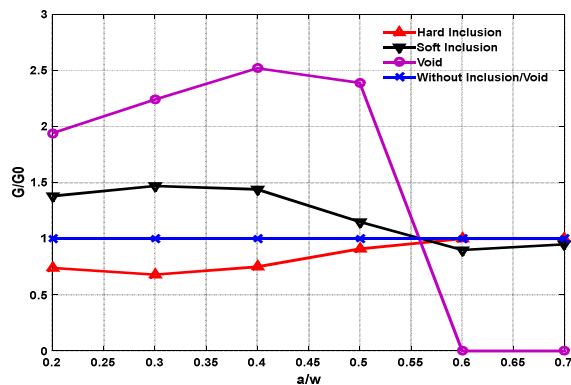

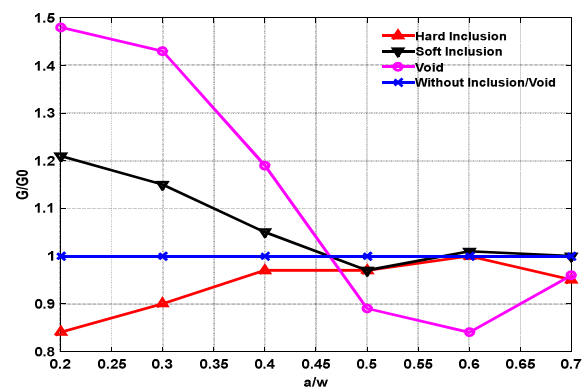**Fig. 32.** Variation of NERR w.r.t. a/w for tensile loading

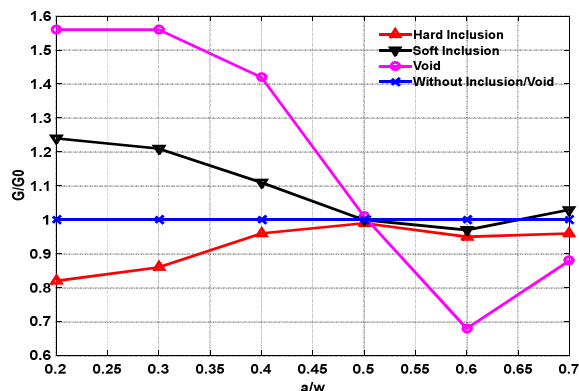**Fig. 33.** Variation of NERR w.r.t a/w for shear loading

Fig. 34. Variation of NERR w.r.t. a/w for combine (Tensile and shear) loading
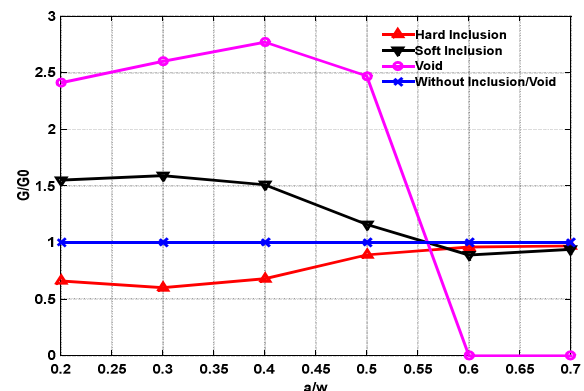

Fig. 35. Variation of NERR w.r.t. a/w for exponential loading

In the present work G/Go for an edge crack plate with inclusions/voids under different loadings is investigated. In Fig. 32 G/Go is calculated for an edge crack plate with inclusions/voids under tensile loading. It is observed that for hard inclusion G/Go decreases as a/w increases up to 0.3 and further increases as a/w increases, whereas for an edge crack isotropic plate with soft inclusion G/Go increases as a/w increases up to 0.3 and further decreases. A similar nature of G/Go is observed for void as for soft inclusion and maximum G/Go ERR is observed at a/w = 0.4. For an edge crack isotropic plate with hard inclusion, as crack advances, it comes near to hard inclusion and due to this G/Go decreases and for further increment, crack deviates its path from hard inclusion and due to this ERR increases. A similar study is carried out for an edge crack isotropic plate with inclusion/void under shear, combined and exponential loading which are as shown in Fig. 33, 34 and 35 respectively.

In Fig. 32, the maximum deviation in G/Go is about 32% and 47% from mean line is observed at a/w=0.3 for an edge crack isotropic plate with hard inclusion and soft inclusion respectively under tensile loading, whereas for cracked plate with void the deviation is more, this is due to the progress of the crack into the void where elastic modulus is negligible.

In Fig. 33, G/Go is calculated for an edge crack isotropic plate with inclusion/void under shear. Here, the maximum deviation in G/Go is about 16%, 21% and 48% from the mean line is observed for hard inclusion, soft inclusion, and void respectively at a/w =0.2. Fig. 34 shows the change of G/Go with respect to a/w for an edge crack isotropic plate with inclusion/void under combined (tensile and shear) loading. Here, the maximum deviation in G/Go is about 18%, 24%,

and 56% is observed for hard inclusion, soft inclusion and void respectively at a/w=0.2.

In Fig. 35, a similar study is carried out for the variation of G/Go with respect to a/w of an edge crack isotropic plate with inclusion/void under exponential loading. From this study, it is observed that the maximum deviation in G/Go is about 40% and 59% from the mean line at a/w= 0.3 for hard and soft inclusion respectively, whereas the maximum deviation in G/Go is more from the mean line at a/w= 0.4 is observed.

4. Conclusions

In the present work, mixed-mode SIF and Energy release rate (ERR) of isotropic edge cracked plate with various discontinuities like crack, voids, soft and hard inclusions numerical were evaluated using XFEM under different loadings. The crack growth with different discontinuities under different loadings (tensile, shear, combine and exponential) was also evaluated. The following observations were found during this numerical investigation study:

- With the increase of crack length, MMSIF increases for voids and/or inclusions under different loadings.
- An isotropic plate with discontinuities like edge crack, void and inclusion are found more sensitive under shear and compound loading.
- The Fracture behavior of the plate with crack and voids/inclusions at near to crack tip is more sensitive.
- With the increase of the number of voids, the MMSIF increases, while decreases for hard inclusions under different loadings.
- The MMSIF is more affected by the position variation of voids/inclusions along the length as compared to the width.
- Crack propagation is straight when void/inclusion is aligned with crack for tensile and exponential loading. Crack propagation is getting deviated downward for the plate without void/inclusion under shear and combined loading.
- The crack propagation is getting deviated towards the hole and soft inclusion and away from hard inclusion. When the crack is get interacted with hard inclusion, the first mode SIF decrease as crack reaches near to it and then increases as crack goes away from it under different loadings. It is because of the hard inclusion is having to harden material properties as compared to plate material.
- As the crack reaches near to hard inclusion NERR decreases and further increases as crack goes away from hard inclusion. When the crack is getting interacted with void reverse nature is observed as of hard inclusion.
- This analysis is helpful to predict the material strength in design the structure with the presence of various discontinuities under different loading conditions.

Conflict of Interest

Funding

References

[1] G. C. Sih, Energy-density concept in fracture mechanics, *Engineering Fracture Mechanics*, 5 (1973) 1037-1040.

[2] J. S. Ke and H. W. Liu, The measurements of fracture toughness of ductile materials, *Engineering Fracture Mechanics*, 5 (1973) 187-202.

[3] W. Z. Chien, Z. C. Xie, Q. L. Gu, Z. F. Yang and C. T. Zhou, The superposition of the finite element method on the singularity terms in determining the stress intensity factor, *Engineering Fracture Mechanics*, 16 (1982) 95-103.

[4] T. Belytschko, H. Chen, J. Xu, and G. Zi, Dynamic crack propagation based on loss of hyperbolicity and a new discontinuous enrichment. *International Journal of Numerical Methods in Engineering*, 58 (2003) 1873–1905.

[5] N. Sukumar and J.H. Prevost, Modelling quasi-static crack growth with the extended finite element method, Part –I, computer implementation, *International Journal of Solids and Structures*, 40 (2003) 7513-7537.

[6] J. Bellec andJ.E. Dolbow, A note on enrichment functions for modeling crack nucleation, *Communications in Numerical Methods in Engineering*, 19 (2003) 921–932.

[7] T. Belytschko, R. Gracie and G.A. Ventura, A review of extended/generalized finite element methods for material modeling, *International Journal of Fracture*, 131 (2005) 124–129.

[8] A. Asadpoure, S. Mohammadi and A. Vafaia, Modelling crack in orthotropic media using a coupled finite element and partition of unity methods, *Finite Elements in Analysis and Design*, 42 (2006) 1165 – 1175.

[9] Z. LI and Q. Chen, Crack- inclusion interaction for mode I crack analyzed by Eshelby equivalent inclusion method, *International Journal of Fracture*, 118 (2002) 29–40.

[10] S.E. Mousavi and N. Sukumar, Generalized Gaussian quadrature rules for discontinuities and crack singularities in the extended finite element method, *Computer Methods in Applied Mechanics and Engineering*, 199 (2010) 3237-3249.

[11] S. Kumar, I.V. Singh, B.K. Mishra and A. Singh, New enrichments in XFEM to model dynamic crack response of 2-D elastic solids, *International Journal of Impact Engineering*, 87 (C) (2016) 198-211.

[12] T. Belytschko and R. Gracie, XFEM applications to dislocations and interfaces, *International Journal of Plasticity*, 23 (10–11) (2007) 1721-1738.

[13] N. Sukumar, D.L. Chop, N. Moes and T. Belytscko, Modelling holes and inclusions by level set in the extended finite element method, *Comp. Methods Apll. Mech.*, 190 (2001) 6183-6200.

[14] W. Limtrakarn and P. Dechaumphai, Adaptive finite element method to determine K_I and K_{II} of crack plate with different $E_{INCLUSION}/E_{PLATE}$ ratio, *Transactions of the Canadian Society for Mechanical Engineering*, 35 (3) (2011) 355-368.

[15] S. Jiang, C. Du, and C. Gu, An investigation into the effects of voids, inclusions and minor cracks on major crack propagation by using XFEM, *Structural Engineering and Mechanics*, 49 (5) (2014) 597-618.

[16] S. Natarajan, P. Kerfriden, D. R. Mahapatra and S. P. A. Bordas, Numerical analysis of the inclusion-crack interaction by the Extended Finite Element Method, *International Journal for Computational Methods in Engineering Science and Mechanics*, 15 (2014) 26–32.

[17] K. Sharma, Crack Interaction Studies Using XFEM Technique, *Journal of Solid Mechanics,* 6 (4) (2014) 410-421.

[18] A. S. Shedbale, I. V. Singh and B. K. Mishra, Nonlinear Simulation of an Embedded Crack in the Presence of Holes and Inclusions by XFEM, *Procedia Engineering*, 64 (2013) 642 – 651.

[19] J. Grasa, J. A. Bea, J. F. Rodriguez, and M. Doblare, The perturbation method, and the extended finite element method. An application to fracture mechanics problems, *Fatigue Fract. Engng. Mater. Struct.*, 29 (2006) 581–587.

[20] K. Khatri and A. Lal, Stochastic XFEM fracture and crack propagation behavior of an isotropic plate with hole emanating radial cracks subjected to various in-plane loadings, *Mechanics of Advanced Materials and Structures*, 25 (9) (2018) 732-755.

[21] K. Khatri and A. Lal, Stochastic XFEM based fracture behavior and crack growth analysis of a plate with a hole emanating cracks under biaxial loading, *Theoretical and Applied Fracture Mechanics*, 96 (2018) 1–22.

[22] M.T. Ebrahimi, D. Dini, D.S. Balint, A.P. Sutton, and S. Ozbayraktar, Discrete crack dynamics: A planar model of crack propagation and crack-inclusion interactions in brittle materials, *International Journal of Solids and Structures*, 152 (2018) 12-27.

[23] K. Huang, L. Guo and H. Yu, Investigation of mixed-mode dynamic stress intensity factors of an interface crack in bi-materials with an inclusion, *Composite Structures*, 202 (2018) 491-499.

[24] T. Yu and T.Q Bui, Numerical simulation of 2-D weak and strong discontinuities by a novel approach based on XFEM with local mesh refinement, *Composite Structures*, 196 (2018) 112-133.

[25] J. Zhang, Z. Qu, Q. Huang, L. Xie, and C. Xiong, Interaction between cracks and a circular inclusion in a finite plate with the distributed dislocation method, *Arch. Appl. Mech.*, 83 (2013) 861–873.

[26] I.V. Singh, B.K. Mishra, S. Bhattacharya, and R.U. Patil, The numerical simulation of fatigue crack growth using extended finite element method, *International Journal of Fatigue*, 36 (2012) 109–119.

[27] A. Lal, S.P. Palekar, S.B. Mulani and R.K. Kapania, Stochastic extended finite element implementation for fracture analysis of laminated composite plate with a central crack, *Aerospace Science and Technology*, 60 (2017) 131-151.

[28] S. Kumar, I.V. Singh, B.K. Mishra, and T. Rabczuk, Modeling, and simulation of kinked cracks by virtual node XFEM, *Computer Methods in Applied Mechanics and Engineering*, 283 (2015) 1425-1466.

[29] T.Q. Bui and C. Zhang, Extended finite element simulation of stationary dynamic cracks in piezoelectric solids under impact loading, *Computational Materials Science,* 62 (2012) 243-257.

[30] Z.H. Teng, D.M. Liaoa, S.C. Wu, F. Sun, T. Chen and Z.B. Zhang, An adaptively refined XFEM for the dynamic fracture problems with micro defects, *Theoretical and Applied Fracture Mechanics*, 103 (2019) 102255.

[31] Z. Han, D. Weatherley and R. Puscasu, A relationship between tensile strength and loading stress governing the onset of mode I crack propagation obtained via numerical investigations using a bonded particle model, *Int. J. Numer. Anal. Meth. Geomech.*, 10 (2017) 1–13.

[32] J. Zhao, Modeling of Crack Growth Using a New Fracture Criteria Based Peridynamics, *J. Appl. Comput. Mech.,* 5(3) (2019) 498-516.

[33] X. Sun, G. Chaia and Y. Bao, Nonlinear numerical study of crack initiation and propagation in a reactor pressure vessel under pressurized thermal shock using XFEM, F*atigue Fract. Eng. Mater. Struct.,* 10 (2017) 1–13.

[34] J.M. Sim and Y.S. Chang, Crack growth evaluation by XFEM for nuclear pipes considering thermal aging embrittlement effect, *Fatigue Fract. Eng. Mater. Struct.,* 11 (2018) 1–17.

[35] D. Wilson, Z. Zheng and F.P.E. Dunne, A microstructure-sensitive driving force for crack growth, *Journal of the Mechanics and Physics of Solids,* 121 (2018) 1–41.

[36] M. Surendran, A.L.N. Pramod and S. Natarajan, Evaluation of Fracture Parameters by Coupling the Edge-Based Smoothed Finite Element Method and the Scaled Boundary Finite Element Method, *J. Appl. Comput. Mech.,* 5(3) (2019) 540-551.

[37] Z. Sun, X. Zhuang and Y. Zhang, Cracking Elements Method for Simulating Complex Crack Growth, *J. Appl. Comput. Mech.,* 5(3) (2019) 552-562.

[38] M. Francesco Funari, P. Lonetti and S. Spadea, A crack growth strategy based on moving mesh method and fracture mechanics, *Theoretical and Applied Fracture Mechanics,* 102 (2019) 1-39.

[39] J.L. Curiel-Sosa, B. Tafazzolimoghaddam, and C. Zhang, Modelling fracture and delamination in composite laminates energy release rate and interfacial stress, *Composite Structures,* 189 (2018) 641-647.

[40] D. Roberto and L. Ma, Energy Release Rate of Moving Circular-Cracks, *Engineering Fracture Mechanics,* 213 (2019)

118-130.

[41] A.M. Aguirre-Mesa, D. Ramirez-Tamayo, M.J. Garcia, A. Montoya, and H. Millwater, A stiffness derivative local hypercomplex-variable finite element method for computing the energy release rate, *Engineering Fracture Mechanics,* 218 (2019) 106581.

[42] R.U. Patil, B.K. Mishra, and I.V. Singh, A new multiscale XFEM for the elastic properties evaluation of heterogeneous materials, *International Journal of Mechanical Sciences*, 122 (2017) 277-287.

[43] S.Z. Feng and W. Li, An accurate and efficient algorithm for the simulation of fatigue crack growth based on XFEM and combined approximations, *Applied Mathematical Modelling*, 55 (2018) 600-615.

[44] S.Z. Feng and X. Han, A novel multi-grid based reanalysis approach for efficient prediction of fatigue crack propagation, *Computer Methods in Applied Mechanics and Engineering,* 353 (2019) 107-122.

[45] T.Q. Bui and C. Zhang, Analysis of generalized dynamic intensity factors of cracked magnetoelectroelastic solids by X-FEM, *Finite Elements in Analysis and Design,* 69 (2013) 19-36.

[46] X. Zhang and T.Q. Bui, A fictitious crack XFEM with two new solution algorithms for cohesive crack growth modeling in concrete structures, *International Journal for Computer Aided Engineering and Software,* 32 (2015) 473-497.

[47] Z. Kang, T. Quoc Bui, D. Dinh Nguyen, T. Saitoh, and S. Hirose, An extended consecutive-interpolation quadrilateral element (XCQ4) applied to linear elastic fracture mechanics, *Acta Mechanica,* 226 (2015) 3991-4015.

[48] Z. Wang, T. Yu, T. Quoc Bui, N. Anh Trinh, N.T. Hien Luong, N. Dinh Duc, and D. Hong Doan, Numerical modeling of 3-D inclusions and voids by a novel adaptive XFEM, *Advances in Engineering Software,* 102 (2016) 105-122.

[49] Z. Kang, T. Quoc Bui, D. Dinh Nguyen and S. Hirose, Dynamic stationary crack analysis of isotropic solids and anisotropic composites by enhanced local enriched consecutive-interpolation elements, *Composite Structures,* 180 (2017) 221-233.

[50] Z. Kang, T. Quoc Bui, T. Saitoh, and S. Hirose, Quasi-static crack propagation simulation by an enhanced nodal gradient finite element with different enrichments, *Composite Structures,* 180 (2017) 221-233.

[51] Z. Wang, T. Yu, T. Quoc Bui, S. Tanaka, C. Zhang, S. Hirose, and J.L. Curiel-Sosa, 3-D local mesh refinement XFEM with variable-node hexahedron elements for extraction of stress intensity factors of straight and curved planar cracks, *Computer Methods in Applied Mechanics and Engineering,* 313 (2017) 375-405.

[52] Z. Kang, T. Quoc Bui, T. Saitoh and S. Hirose, Multi-inclusions modeling by adaptive XIGA based on LR B-splines and multiple level sets, *Finite Elements in Analysis and Design,* 148 (2018) 48-66.

[53] N. Sukumar, D.L. Chopp, N. Moës and T. Belytschko, Modelling holes and inclusions by level sets in the extended finite-element method, *Comput. Methods Appl. Mech. Eng.*, 190 (2001) 6183–6200.

[54] M. Stolarska, D.L. Chopp, N. Moës and T. Belytschko, Modelling crack growth by level sets in the extended finite element method, *Int. J. Numer. Methods Eng.*, 51 (2001) 943–960.

[55] S. Mohammadi, *Extended Finite Element Method for Fracture Analysis of Structures*, Wiley/Blackwell, 2008.

ORCID iD

Achchhe Lal https://orcid.org/0000-0001-7496-2112
Manoj B. Vaghela https://orcid.org/0000-0001-9803-0475
Kundan Mishra https://orcid.org/0000-0001-7802-0982

Publisher's Note Shahid Chamran University of Ahvaz remains neutral with regard to jurisdictional claims in published maps and institutional affiliations.